# SVD applied to Statistical Downscaling for Prediction of Monthly Mean Land Surface Temperatures: Model Documentation.

**DNMI**
Det norske meteorologiske institutt

Rasmus E. Benestad

KLIMA

# DNMI-REPORT

**NORWEGIAN METEOROLOGICAL INSTITUTE**
P.O. BOX 43 BLINDERN, N - 0313 OSLO
TELEPHONE: (+47) 22 96 30 00

TITLE:

## SVD applied to Statistical Downscaling for Prediction of Monthly Mean Land Surface Temperatures: Model Documentation.
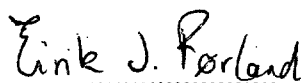
AUTHOR:

**Rasmus E. Benestad**

SUMMARY:

Singular Vector Decomposition (SVD) analysis is discussed as a method for constructing linear downscaling models. A mathematical formulation of the SVD models is derived, and an evaluation of the SVD based predictions is presented, employing sea surface temperatures (SSTs), sea level pressure (SLP), and 500 hPa geopotential heights and temperatures. Cross-validation analyses of the model predictions indicate that the SVD models gave similar results as models based on the Canonical Correlation Analysis (CCA) technique, although the SVD models did not obtain as high correlation scores as the CCA models. The SVD models with the highest skill scores were based on 500 hPa temperatures, suggesting that the upper air temperatures are promising predictor candidates for statistical downscaling.

SIGNATURES:

**Eirik J. Førland**
Principal Investigator, RegClim-PT3

**Bjørn Aune**
Head of the DNMI Climate Division

# SVD applied to Statistical Downscaling for Prediction of Monthly Mean Land Surface Temperatures: Model Documentation.

R.E. Benestad

DNMI, December 3, 1998

**Reg Clim**

# Contents

# 1   Introduction

The singular vector decomposition (SVD) analysis is a method for finding coupled spatial patterns which have maximum temporal covariance. The SVD analysis discussed in this report is implemented in the Matlab script, *cmpsvd.m*, and employs a numerical algorithm which calculates left and right eigenvectors (*Press* et al., 1989; *Strang*, 1995). It is important to stress that this numerical algorithm and the coupled pattern analysis described here are two different concepts although both are referred to as SVD. The coupled pattern analysis SVD method (hereafter, referred to as just SVD) is similar to the CCA (*Benestad*, 1998a; *Wilks*, 1995; *Bretherton* et al., 1992; *Preisendorfer*, 1988), but differs from CCA by the fact that the SVD finds spatial patterns with the maximum covariance whereas CCA finds patterns with maximum correlation. In other words, the SVD models are less sensitive to weak signals with high correlation than the CCA models.

The intention of this report is to provide a documentation of the statistical models at *Det Norske Meteorologiske Institutt* (DNMI) based on the SVD method, and to describe the construction and testing of these. This report is the second part of the *Linear Statistical Downscaling Methods* series, and follows up the discussion on Canonical Correlation Analysis (CCA) models in *Benestad* (1998a). We will focus on the *optimal models* which are calibrated on a selection of EOFs that maximise the prediction skill. Since the SVD technique is similar to the CCA method, we will compare the two model classes and discuss the differences in terms of temperature predictions. The purpose of developing these statistical models is to produce regional climate scenarios from given global general circulation model (GCM) results, and we will discuss the suitability of the SVD models for such applications.

In this report, we define *best skill* as the prediction with the highest correlation score. When the comparing between the CCA and SVD models, we also employ mean station scores, i.e. the average skill score of the 24 different stations. A comparison between the average scores is not necessarily a good way of evaluating comparative prediction skill, as both model types may produce very good predictions for a small selection of stations and obtain mediocre and low skill scores for other locations. However, the station mean and variance may provide the basis for a crude significance test of the model differences. Furthermore, the comparison between mean skill scores may give an indication of how well the two model types can predict large scale climate anomalies. Other skill measures include the root mean square errors (RMSE) and proportional variance. The proportional variance score is the ratio of the variance of the predictions to that of the observations, and is a measure of the predicted variance but does not necessarily indicate how

much *of the observed variability* that can be described by the model. For instance, the predictions in some cases were associated with large variance despite being uncorrelated with the observations. The variance score for a prefect prediction, however, is var=100%.

The leading SVD predictor pattern or predictand weights will, unless otherwise stated, hereafter also be referred to simply as "the predictor pattern" and the "predictand weights" respectively.
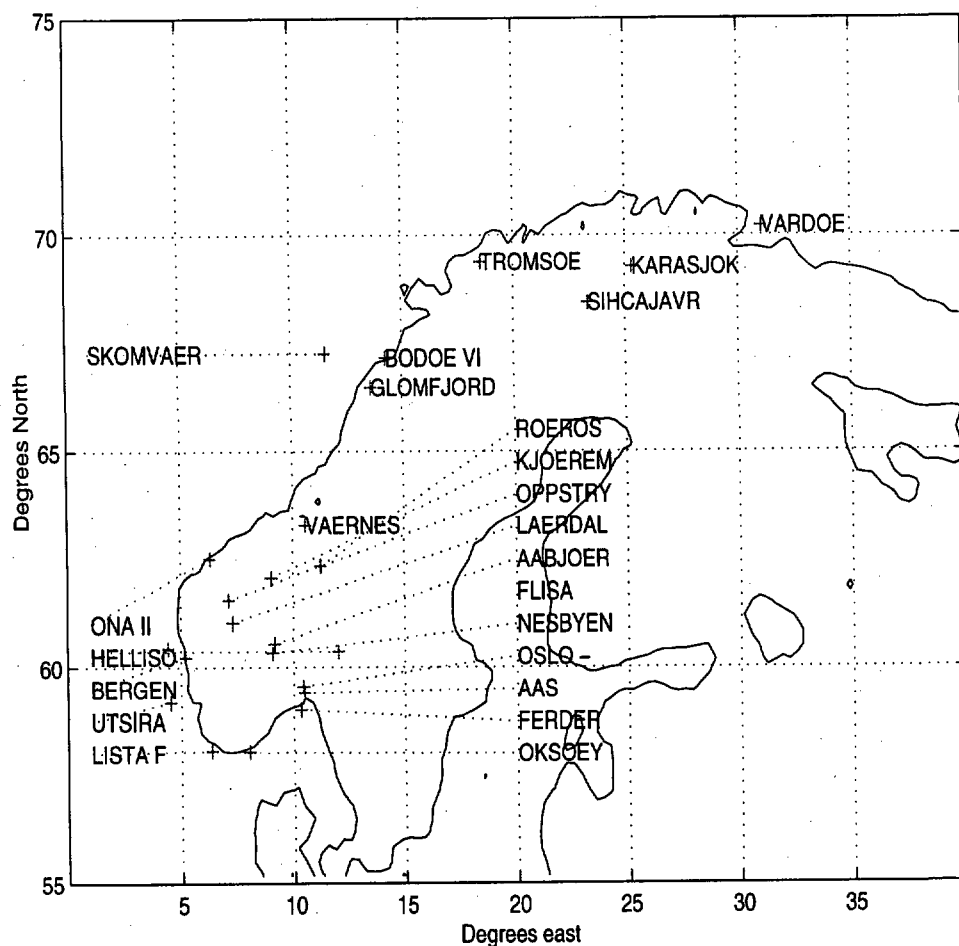
# 2   The SVD Technique

Figure 1: Map showing the location of the the stations (predictand locations) referred to in this report.

The predictors, X, and predictands, Y, described in this report are the same as those in *Benestad* (1998b) and *Benestad* (1998a), with the addition of the 500hPa temperature fields[1]. Figure 1 shows a map of the 24 stations which were included in predictand data set discussed here. We used monthly mean values of land surface temperature[2] from a number of stations, where only stations with long time series were selected, shown in figure 1. 4 stations were located in northern Norway (Vardø, Karasjok, Sihcajarvi and Tromsø), 3 sites were selected from mid Norway (Bodø, Skomvær fyr and Glomfjord), whereas the remaining 18 time series were from the southern part of Norway. There were 9 inland stations (Karasjok, Sihcajarvi, Røros, Kjøremsgrendi, Oppstryn, Lærdal, Åbjørsbråten, Flisa and Nesbyen) and 14 coastal stations. The period spanned by the predictands was 75 years, from 1923 to 1978. The reason why predictand data more up to date were not used in this study was that 1978 was the year that some of the stations with a long temperature record, such as Skomvær fyr, ended. We intend to use the 1978 to 1998 period for the validation of these models later on.

The notations employed here are the same as in *Benestad* (1998a), and the predictor and predictand data can be written as following:

$$Y = G_{svd}U_{svd}^T,$$
$$X = H_{svd}V_{svd}^T, \tag{1}$$

where $U_{svd}$ and $V_{svd}$, often referred to as extension coefficients, describe the temporal evolution of the spatial patterns described by $G_{svd}$ and $H_{svd}$. The matrices $U_{svd}$ and $V_{svd}$ contain the time series of the SVD patterns along their columns so that the leading columns of the two matrices have the greatest possible covariance. We will henceforth drop the subscripts, as all the matrices discussed here are SVD products. Mathematically, the SVD analysis can be posed as a maximization problem, which can be expressed in the form of an eigenvalue equation in a similar fashion as for CCA (*Benestad*, 1998a). The covariance matrix is calculated according to:

$$X^T Y = C_{XY}. \tag{2}$$

The mathematical solution to the maximisation problem is similar to that of CCA, but with $C$ replaced by $C_{XY}$:

---

[1]The $T_{500hPa}$ data were not discussed in the previous report because the $T_{500hPa}$ record was too short for model calibration and the estimate of the square root covariance matrix was complex. The square root covariance matrix is not used in the SVD method. The 500hPa temperature data spanned the period 1962-1994.

[2]Precipitation and other quantities will be discussed in later reports.

$$C_{XY} = LMR^T. \tag{3}$$

The rotation matrices, L and R, represent the actual spatial patterns that have maximum covariance. The expansion coefficients are given by the matrix products (*Bretherton* et al., 1992):

$$U = LY, \tag{4}$$
$$V = RX. \tag{5}$$

The linear relationship between the predictors and predictands employing SVD analysis products is given in equation 6:

$$\hat{Y} = GC_{YV}C_{VV}^{-1}V^T,$$
$$\hat{X} = HC_{XU}C_{UU}^{-1}U^T, \tag{6}$$

In equation 6 we have included the scaling factors $C_{VV}^{-1}$ and $C_{UU}^{-1}$ so that $\hat{Y}$ accounts for as much variance as $Y$. If $X = Y$, then $G \equiv H$, $V \equiv U$ and $X = HC_{XU}C_{UU}^{-1}U^T = HU^T$, which implies[3] that $C_{XU} = C_{UU} = C_{XX}$. The singular value decomposition extension coefficients can be expressed in terms of the spatial SVD patterns and the original data, $V^T = H^TX$, and the first equations in 6 can therefore be expressed as:

$$\hat{Y} = GMC_{XX}^{-1}V^T,$$
$$\hat{Y} = GMC_{XX}^{-1}H^TX = \Psi X, \tag{7}$$

where $M = C_{XY}$. The SVD time series, U and V, have similar variance as Y and X respectively, and the singular vectors (spatial patterns) satisfy $G^TG = H^TH = I$. The expression for $\Psi$ can be obtained from equation 7, where $\Psi = GMC_{XX}^{-1}H^T$. The Matlab script *cmpsvd.m* estimates the SVD products and the linear model $\Psi$. The optimal predictor combination was found, as in *Benestad* (1998a), by a screening method where only the EOFs that increased the cross-validation correlation scores were included in the optimal models.

---

[3]$X^TU = U^TU \rightarrow X = U \rightarrow X^TX = U^TU$.

# 3   SST Models

Two types of SST models will be discussed here. The first kind is a model calibrated with regional SSTs covering the area 10°W to 40°E and 55°N to 75°N, which will be referred to as the 'Nordic Seas model', including SSTs from the North Sea, Barents Sea, the Norwegian Sea, Skagerrak, Kattegat, and the Baltic Sea (figure 4). The second model type covers a larger area, 90°W to 40°E and 15°N to 80°N, and is called the 'North Atlantic model', although the North Sea, Mediterranean, the Black Sea, the Labrador Sea, the Barents Sea, the Norwegian Sea, Skagerrak, Kattegat, the Baltic Sea, and Hudson Bay also are included (figure 13).

Figures 2 and 3 show the cross-validation predictions for two SVD models which included different EOF combinations as predictors in the model calibration and prediction. The results from the *optimal* SVD model, i.e. the SVD model based on the EOF combination which gave the maximum correlation scores for the best of model prediction of the 24 stations, are shown in figure 2. The results of an SVD model using the same optimal EOF combination as the corresponding optimal CCA model described in *Benestad* (1998a), henceforth referred to as the CCASVD model, are shown in figure 3. Table 1 indicates that the predictions of the optimal SVD model included EOFs 1, 2, 5, 10, 11, 18 and 19 while the corresponding optimal CCA model was based on EOFs 1, 2, 3, 6, 7 and 8.

The best predictions of the January SVD model was found for stations with continental climate type such as Oslo and Flisa (figures 4 and 6, left panel) while the CCASVD and the CCA models gave best predictions for Ferder fyr which has a coastal climate (figure 4 and 6, right panel). The CCA technique identified the stations and SST patterns with the highest correlation, which in this case were the SST anomalies in Skagerrak and Kattegat and the adjacent coastal temperatures (figure 6, right panel), and did not take into account the strength of the signal. The SVD models, on the other hand, put more emphasis on the strong signals and was less sensitive to weak signals with high correlation. The CCASVD model was a hybrid between the CCA and SVD model, using the SVD technique to find the patterns with maximum covariance, given the the optimal CCA EOF predictor combination.

The fact that the CCASVD model produced best predictions for the Ferder fyr and the SVD model obtained best scores for Flisa suggests that SST anomalies in different regions were connected with the temperatures in different parts of Norway. The difference between the leading SVD and CCASVD predictor patterns is shown in figure 5 (bottom panel), and the geographical shift in prediction skill appeared to be associated with small

scale SST anomalies south of Svalbard, along the Barents Sea coast of Kola, in the Baltic, and more extensive SST anomalies north of Scotland. The coastal SST anomalies may have been a result of upwelling due to the local wind direction, and the fact that these were only small scale features also suggest that they had little significance for the Norwegian January temperatures. It seems more likely that the extensive SST anomalies north of Scotland affected the Norwegian temperatures. However, the question of causality can only be resolved through numerical experiments employing physical and dynamical models.

The January SST CCASVD model scored lower with respect to the correlation skill (Ferder fyr: 0.65) than the corresponding CCA predictions for the same location and based on the same predictor combinations (*Benestad* (1998a): r=0.72). The January CCA predictions were associated with 60% (Ferder fyr) of the total variance at Ferder fyr while the SVD predictions 'accounted' for 61% (in Oslo) and the CCASVD model described 89% (Ferder fyr).

It is apparent from the Nordic Seas SST model results that the SVD model gave high prediction scores for only one or two of the stations while the CCA method produced skillful predictions for several locations (figures 6, 10 and 14). Furthermore, the 'worst' predictions of several of the SST SVD models were associated with negative cross-validation correlation coefficients while only the October SST CCA models gave such bad predictions. The difference in worst correlation scores between the SVD and CCASVD models for January temperatures was due to the different predictor combinations in the optimal CCA and SVD models, as the CCASVD (figure 6) gave correlation scores which all were higher than zero.

A closer inspection of figures 2 and 3 shows that the January Nordic Seas CCASVD prediction for Ferder fyr in figure 3 captured most of the cold anomalies while the SVD model underestimated the cold event in Oslo (figures 2). The warm months in the 1970s were well captured by the CCASVD model for Ferder fyr but the SVD models underestimated the high temperatures in Oslo. The SST Nordic Seas SVD predictions for April captured most of the cold anomaly at Ås, but nevertheless gave mediocre overall correlation and RMSE scores (figure 7). In July, the SVD model produced best prediction for Oppstryn, but the prediction could only 'account for' 22% of the temperature variability (figure 8). The October prediction for Oksøy fyr, shown in figure 11, 'described' nearly 100% of the variability, although the model did not predict the cold events at the right times and the correlation and RMSE skill scores were low.

Although the correlation score for the best January SST SVD model prediction was higher than the best CCASVD score, the mean cross-validation
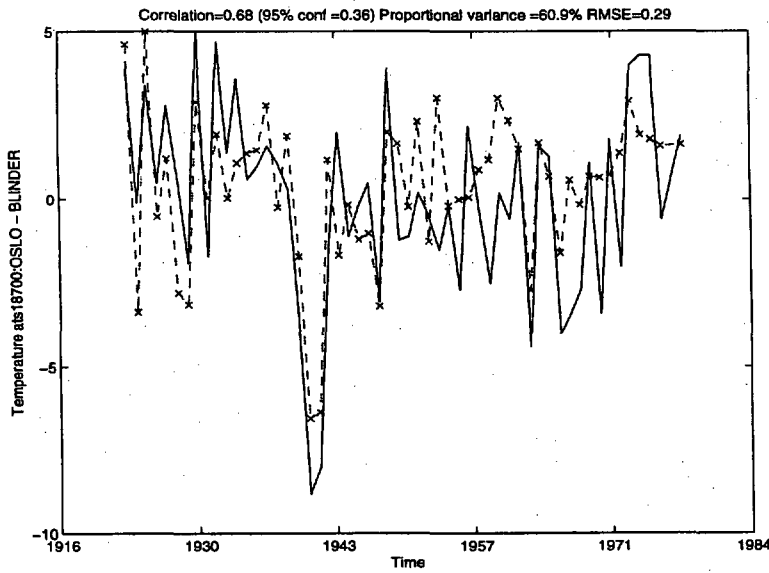
Figure 2: Time series of predicted January temperatures (dashed) at Oslo, employing the cross-validation method with GISST2.2 Nordic Seas SSTs, shown with the observations (black solid line).
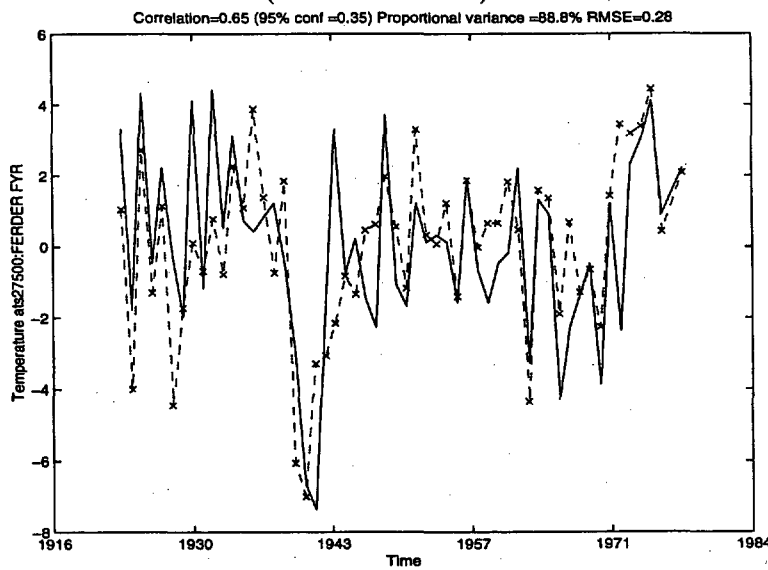


Figure 3: Same as figure 2, but using the same EOF combination as the corresponding optimal CCA model. The time series represents the January temperatures from Ferder fyr, as opposed to Oslo in figure 2.
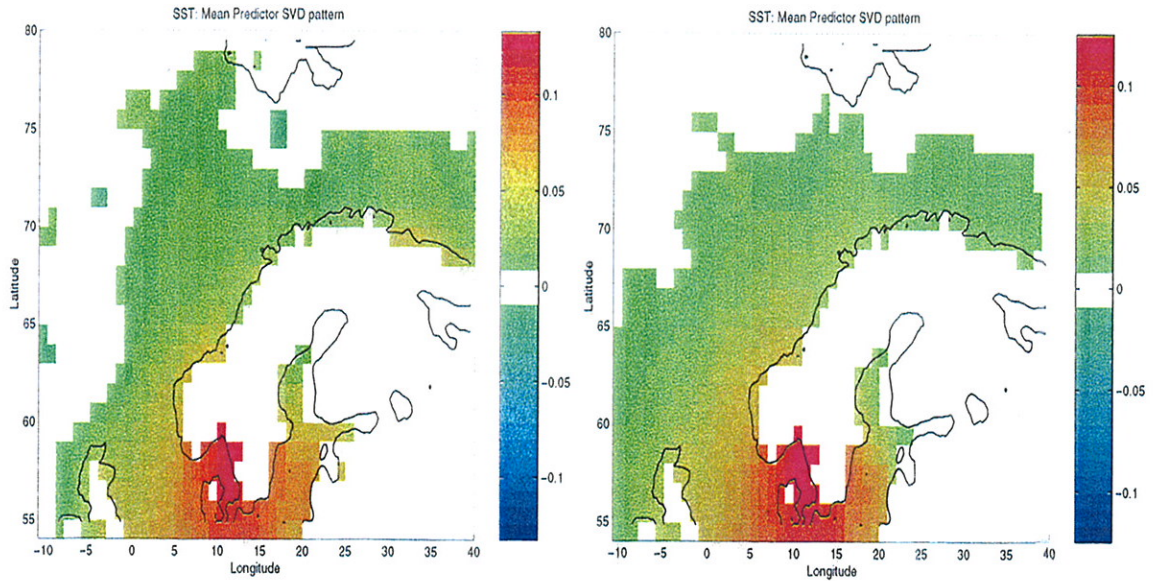
Figure 4: The mean leading January SVD GISST2.2SST pattern associated with the land surface temperature. The left panel shows the SVD pattern for the optimal SVD model while the right panel shows the CCASVD predictor pattern.
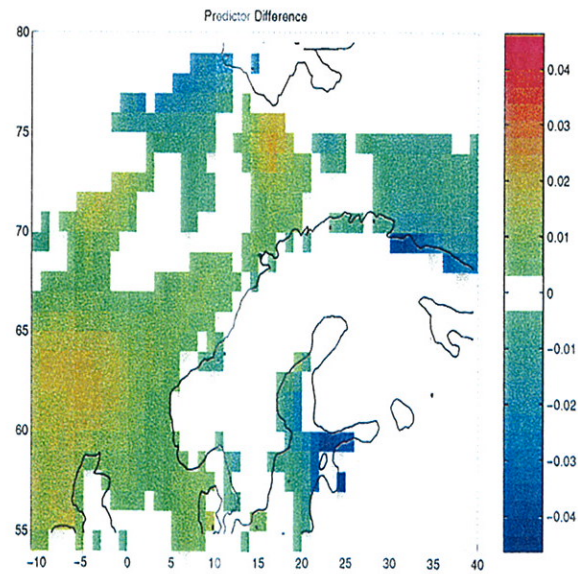


Figure 5: The difference between the two predictor patterns (The right panel minus the left panel) in figure 4 may indicate in which locations the SST anomalies determine whether the models are optimised for Ferder fyr or Oslo.

The 1st SVD weights of the station data

| Station | Cor | Var(%) | RMSE |
|---|---|---|---|
| s98550:VARDOE | 0.07 | 123 | 0.3 |
| s97250:KARASJOK | 0.10 | 12 | 0.6 |
| s93900:SIHCAJAVRI | 0.27 | 22 | 0.5 |
| s90450:TROMSOE | −0.16 | 54 | 0.3 |
| s85950:SKOMVAER FYR | 0.03 | 116 | 0.3 |
| s82290:BODOE VI | 0.42 | 35 | 0.3 |
| s80700:GLOMFJORD | 0.27 | 41 | 0.3 |
| s69100:VAERNES | 0.41 | 54 | 0.4 |
| s62480:ONA II | 0.34 | 127 | 0.2 |
| s58700:OPPSTRYN | 0.23 | 36 | 0.3 |
| s54130:LAERDAL - TOEN | 0.45 | 33 | 0.4 |
| s52530:HELLISOEY FYR | 0.51 | 96 | 0.2 |
| s50540:BERGEN - FLORI | 0.37 | 41 | 0.3 |
| s47300:UTSIRA FYR | 0.45 | 61 | 0.2 |
| s42160:LISTA FYR | 0.52 | 54 | 0.3 |
| s39100:OKSOEY FYR | 0.55 | 64 | 0.3 |
| s27500:FERDER FYR | 0.44 | 48 | 0.3 |
| s24880:NESBYEN - SKOG | 0.45 | 38 | 0.5 |
| s23160:AABJOERSBRAATE | 0.41 | 53 | 0.4 |
| s18700:OSLO - BLINDER | 0.68 | 61 | 0.3 |
| s17850:AAS | 0.45 | 32 | 0.4 |
| s16740:KJOEREMSGRENDI | 0.40 | 29 | 0.4 |
| s10400:ROEROS | 0.38 | 24 | 0.5 |
| s6040:FLISA | 0.62 | 45 | 0.4 |

Coefficient value in y=ax: a

eof–Jan–Gsst0394–nsea.nc

The 1st SVD weights of the station data

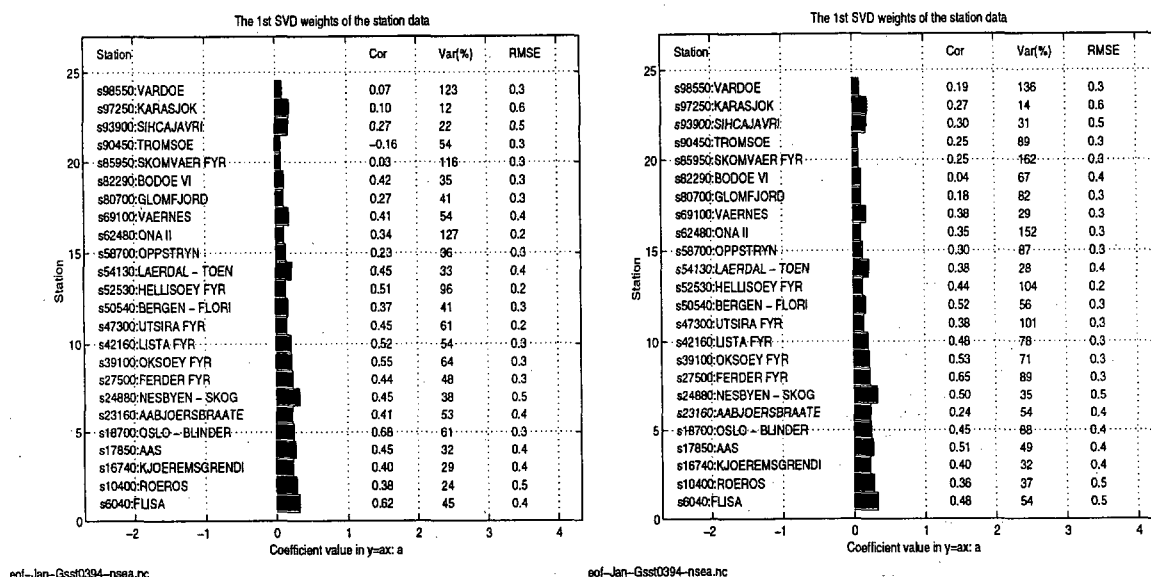| Station | Cor | Var(%) | RMSE |
|---|---|---|---|
| s98550:VARDOE | 0.19 | 136 | 0.3 |
| s97250:KARASJOK | 0.27 | 14 | 0.6 |
| s93900:SIHCAJAVRI | 0.30 | 31 | 0.5 |
| s90450:TROMSOE | 0.25 | 89 | 0.3 |
| s85950:SKOMVAER FYR | 0.25 | 162 | 0.3 |
| s82290:BODOE VI | 0.04 | 67 | 0.4 |
| s80700:GLOMFJORD | 0.18 | 82 | 0.3 |
| s69100:VAERNES | 0.38 | 29 | 0.3 |
| s62480:ONA II | 0.35 | 152 | 0.3 |
| s58700:OPPSTRYN | 0.30 | 87 | 0.3 |
| s54130:LAERDAL - TOEN | 0.38 | 28 | 0.4 |
| s52530:HELLISOEY FYR | 0.44 | 104 | 0.2 |
| s50540:BERGEN - FLORI | 0.52 | 56 | 0.3 |
| s47300:UTSIRA FYR | 0.38 | 101 | 0.3 |
| s42160:LISTA FYR | 0.48 | 78 | 0.3 |
| s39100:OKSOEY FYR | 0.53 | 71 | 0.3 |
| s27500:FERDER FYR | 0.65 | 89 | 0.3 |
| s24880:NESBYEN - SKOG | 0.50 | 35 | 0.5 |
| s23160:AABJOERSBRAATE | 0.24 | 54 | 0.4 |
| s18700:OSLO - BLINDER | 0.45 | 88 | 0.4 |
| s17850:AAS | 0.51 | 49 | 0.4 |
| s16740:KJOEREMSGRENDI | 0.40 | 32 | 0.4 |
| s10400:ROEROS | 0.36 | 37 | 0.5 |
| s6040:FLISA | 0.48 | 54 | 0.5 |

Coefficient value in y=ax: a

eof–Jan–Gsst0394–nsea.nc

Figure 6: The mean January predictand weights shown in filled bars for the land surface temperatures. The correlation results from the cross-validation analysis are given on the right hand side. The left panel shows the results for a model optimised for the SVD method while the right panel shows the result for a corresponding model using CCA optimised predictor combination (*Benestad*, 1998a). The cross-validation correlation, proportional variance and root mean squared error scores are given for each station on the right.

correlation coefficient for all the January Nordic Seas SST SVD predictions in figure 6 were marginally lower than the mean score for the CCASVD prediction ($\overline{r_{svd}}$ = 0.36 and $\overline{r_{ccasvd}}$ = 0.37, with standard deviations of s=0.19 and s=0.14 respectively). The corresponding January mean CCA correlation scores for the same stations was $\overline{r_{cca}}$ = 0.54 (*Benestad*, 1998a) with a standard deviation of s=0.10, which suggests that the CCA model predictions had substantially higher correlation skill than both the SVD and CCASVD models. A simple Student's T-test (*Wilks*, 1995, p.123) confirmed that the mean January CCA correlation scores were higher than the corresponding mean SVD and CCASVD scores at a 95% confidence level (Student's T-test scores of z=4.8 and 4.1 respectively, where a score higher than 2.0 is the criterion for 95% probability that the mean values are different). The same parametric test also revealed that the mean January CCASVD model correlation skill was not significantly higher than the January mean SVD model skill.

The SVD SST models gave lower correlation scores than the CCA models in April and July (figures 7 and 8). The significance test of the station mean correlation scores gave Student's T-test scores of z=6.9 for April and z=5.6 for July (April: $\overline{r_{svd}}$ = 0.12 and $\overline{r_{cca}}$ = 0.45, $s_{svd}$ = 0.16 and $s_{cca}$ = 0.17; July: $\overline{r_{svd}}$ = 0.06 and $\overline{r_{cca}}$ = 0.28, $s_{svd}$ = 0.17 and $s_{cca}$ = 0.09) indicating significantly greater CCA correlation scores. On the other hand, the statistical significance of the difference between the mean correlation scores of the SVD and CCA models for October did not exceed the 95% level ($\overline{r_{svd}}$ = −0.02 and $\overline{r_{cca}}$ = 0.07, with standard deviations of 0.16 and 0.22 respectively, and Student's T-test score of z=1.6).

The January Nordic Seas CCA model 'could account' for 43% (s=8%) of the station mean variance, compared to 54% (s=31%) for the SVD model and 71% (s=40%) for the CCASVD model. Although the SVD models in general predicted more realistic mean variance for all stations, the standard deviation was greater than those for the CCA predictions, making the SVD and CCASVD prediction of the variance for single stations more uncertain than the CCA predictions. Student's T-test statistical significance tests revealed that only the CCA and CCASVD January mean variance predictions were different above the 95% significance limit (z=3.33), and that the January mean variance difference between the SVD and CCASVD (z=1.64) was only significant to the 89% confidence level and the SVD-CCA mean difference (z=1.65) to the 90% limit (*Wilks*, 1995, Table B.1). The same analysis for October (figure 14, left panel) revealed significantly different values for mean variance of the CCA and SVD predictions ($\overline{s_{svd}^2}$ = 101% and $\overline{s_{cca}^2}$ = 23%, with standard deviations of 77% and 7% respectively, and Student's T-test score of z=4.7).
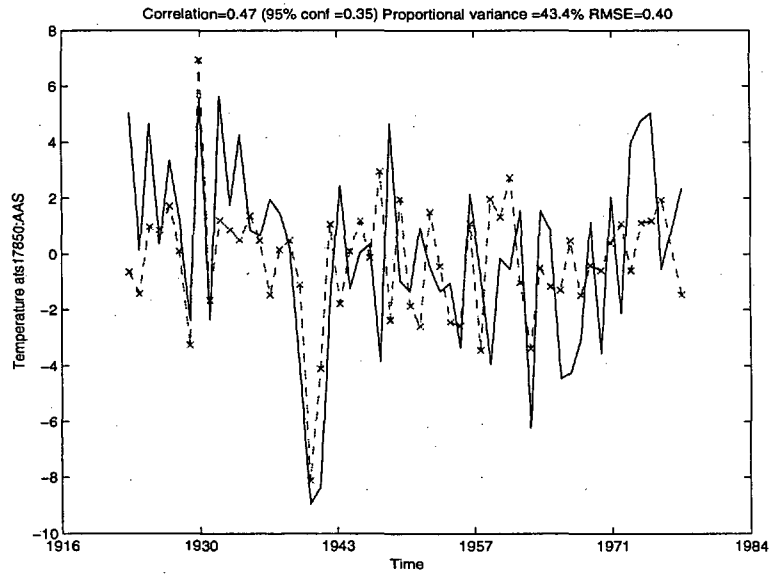
Figure 7: Same as figure 2, but for the April month. The time series represent the temperatures from Ås.
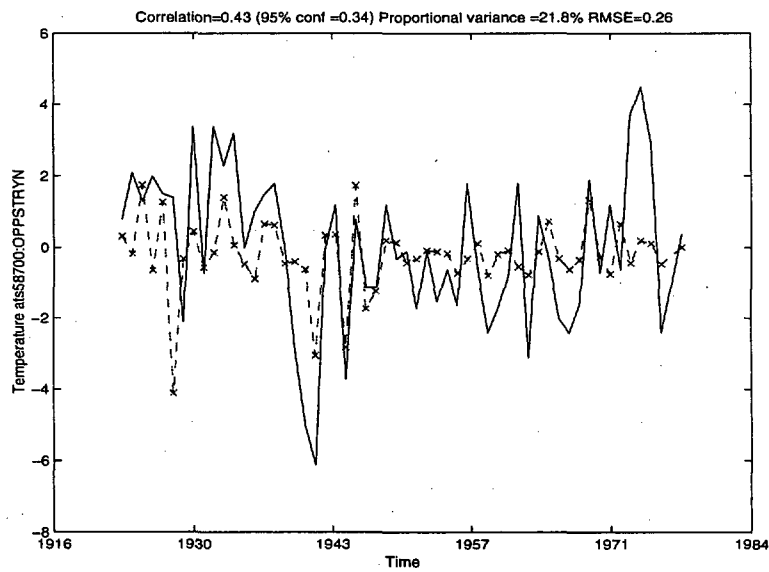


Figure 8: Same as figure 2, but for the July month. The time series represent the temperatures from Oppstryn.
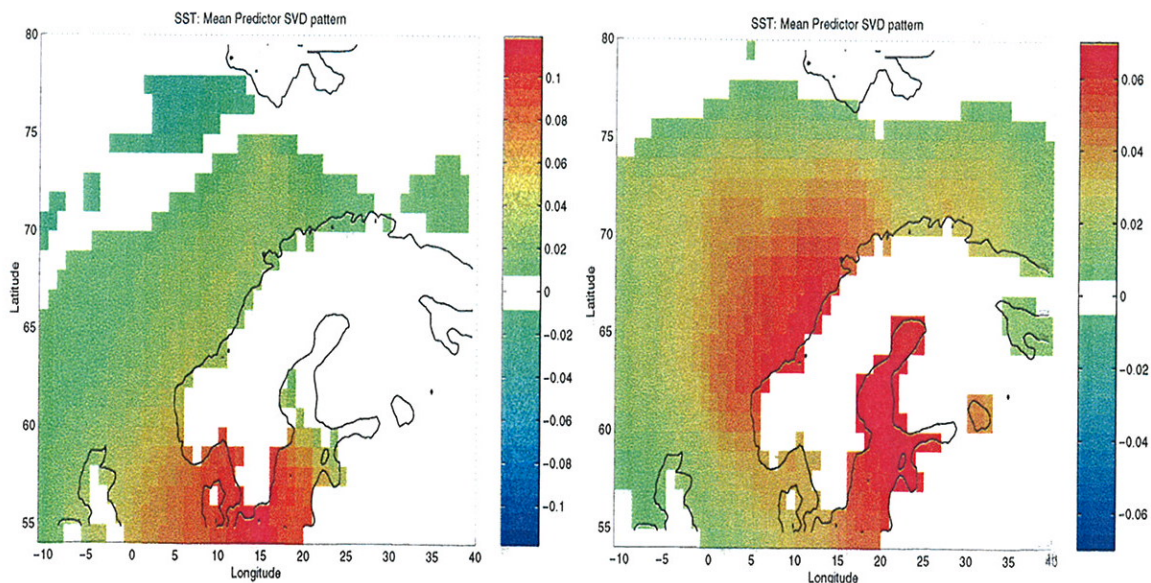
Figure 9: The mean leading April (left) and July (right) SVD GISST2.2 SST predictor pattern associated with the land temperatures.
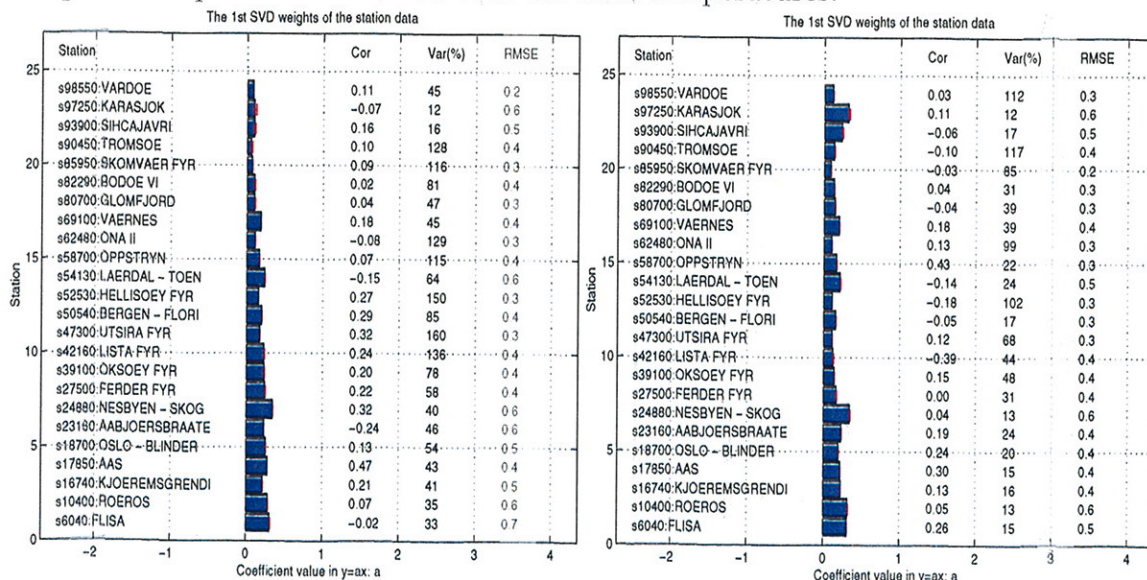


Figure 10: The mean April (left) and July (right) predictand weights shown in filled bars for the land surface temperatures. The correlation results from the cross-validation analysis are given on the right hand side.
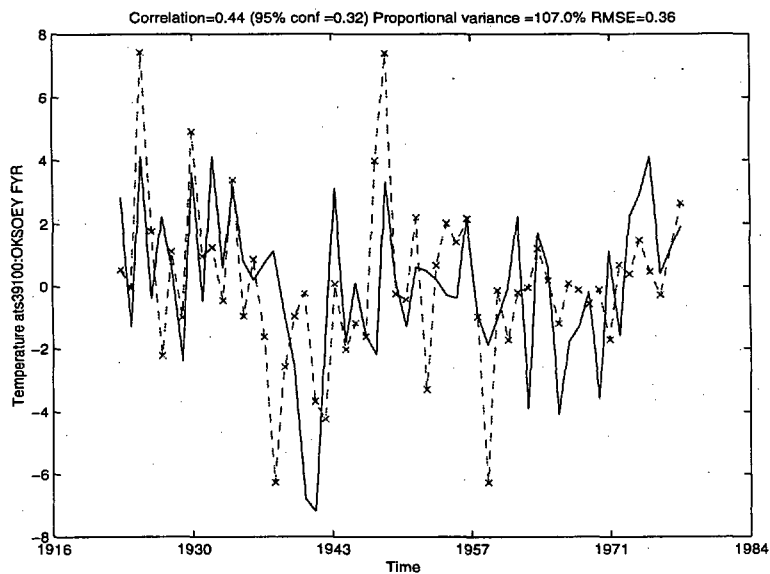
Figure 11: Same as figure 2, but for the October month. The time series represent the temperatures from Oksøy fyr.
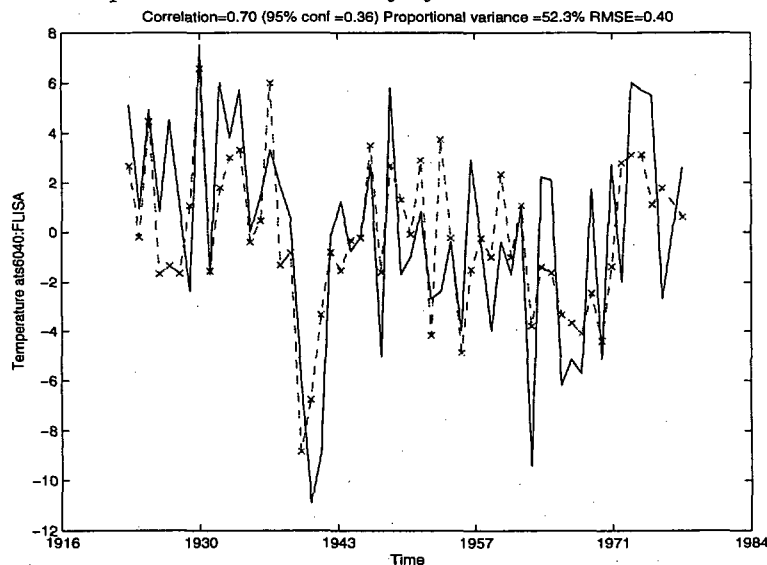


Figure 12: Same as figure 2, but for the North Atlantic January SST model. The time series represent the temperatures from Flisa.
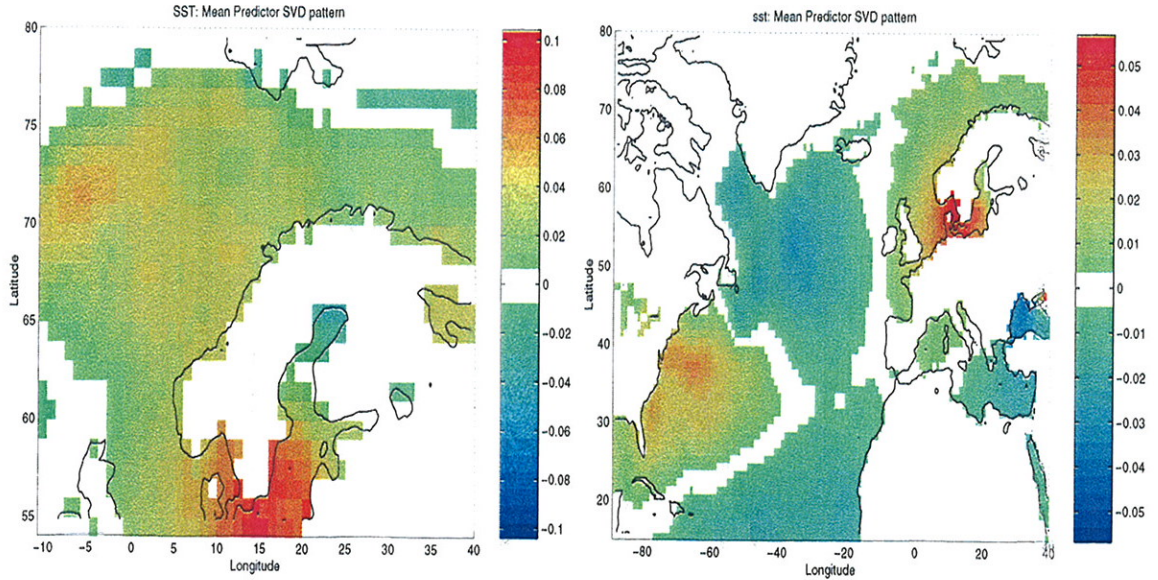
Figure 13: The mean leading October (left) and January North Atlantic (right) SVD GISST2.2SST pattern associated with the land surface temperatures.
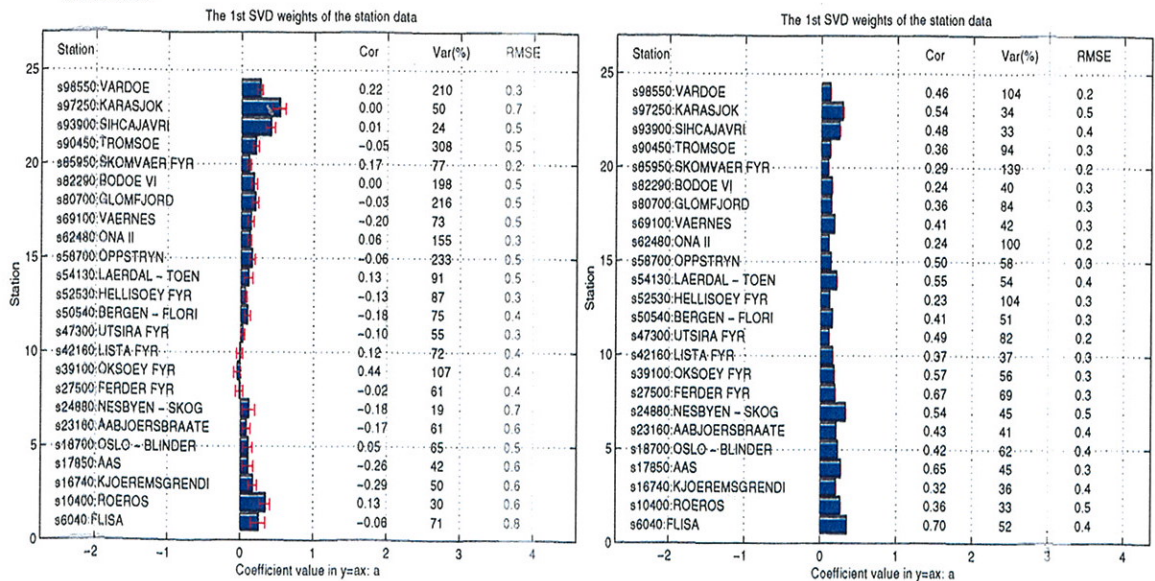


Figure 14: Same as figure 10, but showing the results for the October Nordic Seas (left) and January North Atlantic (right) models.

Figure 12 shows the prediction for Flisa using the *North Atlantic January SVD SST* model, which gave slightly lower correlation skill for Flisa temperatures (r=0.70) than corresponding CCA model (r=0.75). The leading North Atlantic January SST predictor pattern is shown in figure 13 (right panel), and a comparison with the corresponding CCA predictor (*Benestad*, 1998a) pattern revealed similar spatial structures for the two models. The SVD prediction was also associated with smaller variance and higher RMS error than the corresponding CCA prediction (SVD: r=0.70, $s^2$=52%, RMSE=0.40°C figure 14; The CCA correlation score was 0.75, $s^2$=66%, RMSE=0.37°C).

In summary, SVD and CCA SST techniques revealed similar spatial structures for the leading predictor patterns, and models based on both methods were associated with highest prediction scores in January. Neither the SVD nor the CCA models were able to predict July and October temperatures very well. The CCA models was superior to the SVD models for all seasons, but the CCA SST model had some skill during April when the SVD model skill was negligible. The low prediction scores during summer and autumn reflects the weak connection between the SSTs and the land temperatures during these seasons. A physical explanation for a seasonally varying SST influence on the monthly mean temperatures may be that the advection of warm air from maritime regions is an important warming mechanism during January with strong atmospheric circulation and that variations in local radiation budget (clouds) is the dominant term during the seasons when the atmospheric circulation is weak. It is also possible that the atmosphere-ocean coupling is weaker during summer and autumn, however, persistence studies of air temperatures (south of Labrador Sea) suggest strongest coupling during April, not in January (*Bhatt* et al., 1998).

The smaller SVD predictand and predictor weights than the corresponding CCA weights reflect the fact that in the SVD analysis the spatial patterns are normalised and the time series account for the signal variance, while for the CCA it is the time series which are normalised and the spatial patterns which describe the signal variance.

# 4 SLP Models

## 4.1 The NMC ds195.5 models

The cross-validation results for the NMC SLP SVD models are shown in figures 15 to 23. Although the scores suggest that the SVD models were skillful with correlation scores higher than 0.66, they were inferior to the CCA models with respect to correlation scores and RMS errors. (Highest
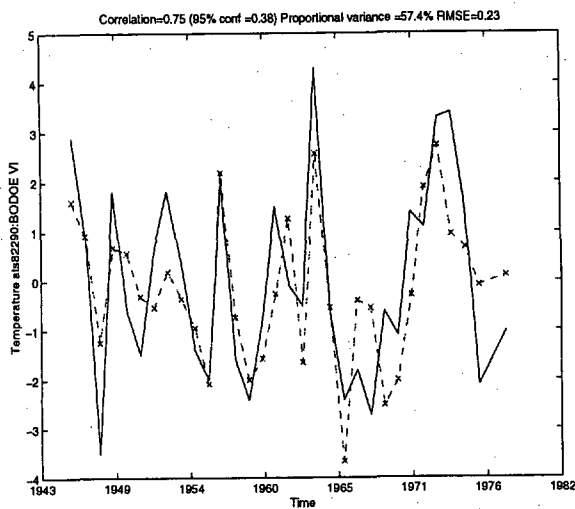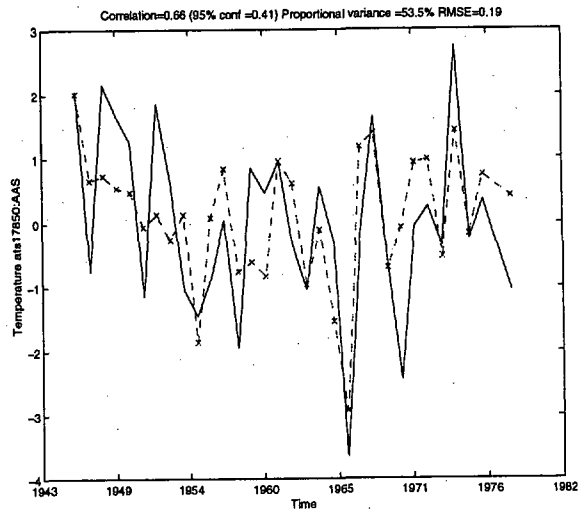
Figure 15: Time series of predicted January (left) and April (right) temperatures (dashed) at Bodø (left) and Ås (right), employing the cross-validation method with NMC SLPs, shown with the observations (black solid line).
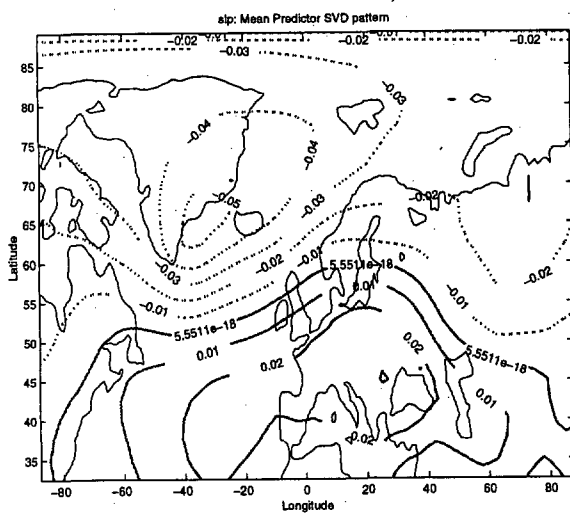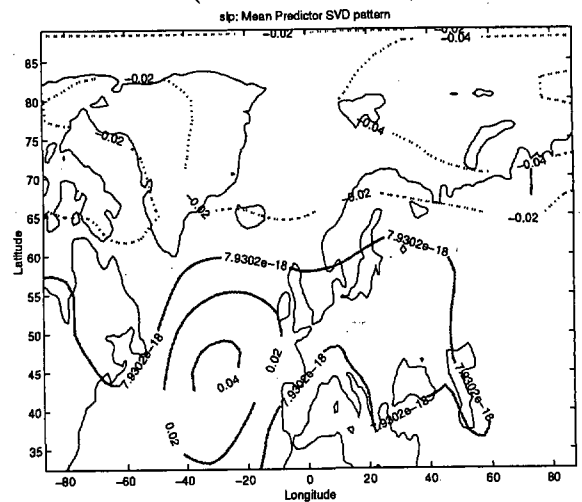


Figure 16: The mean leading January (left) and April (right) SVD NMC SLP patterns associated with the land surface temperatures.
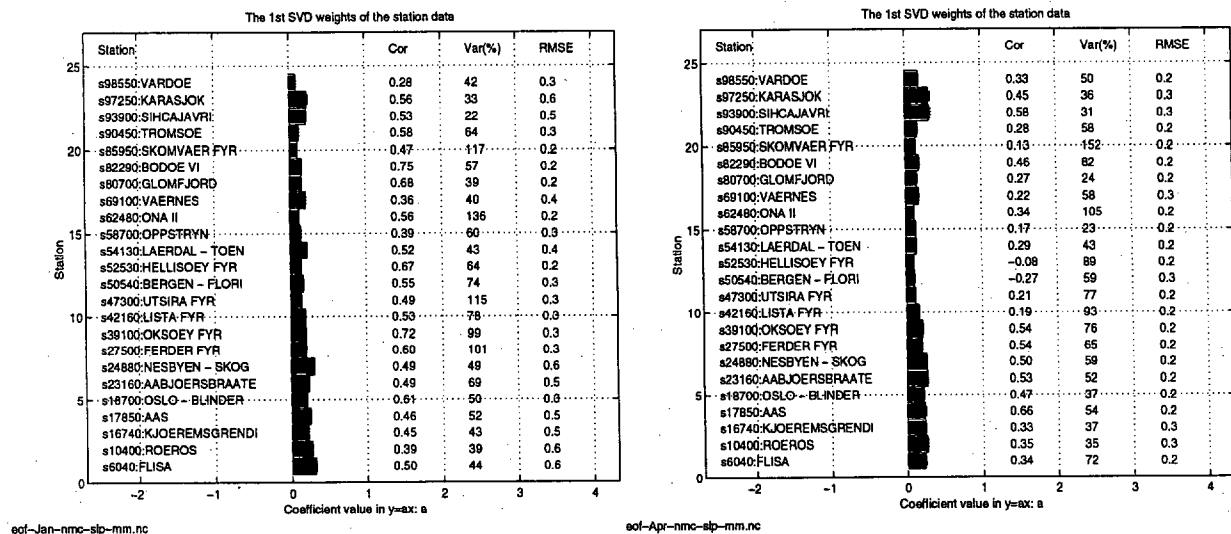
**Figure 17:** The mean leading January (left) and April (right) weights from the cross-validation analysis shown in filled bars indicate the mean SVD predictand weights for the land surface temperatures. The empty black boxes show the weights from a model trained on the whole time series. The error bars indicate the standard deviation and hence the spread in samples of each coefficient. The correlation results from the cross-validation analysis are given on the right hand side.
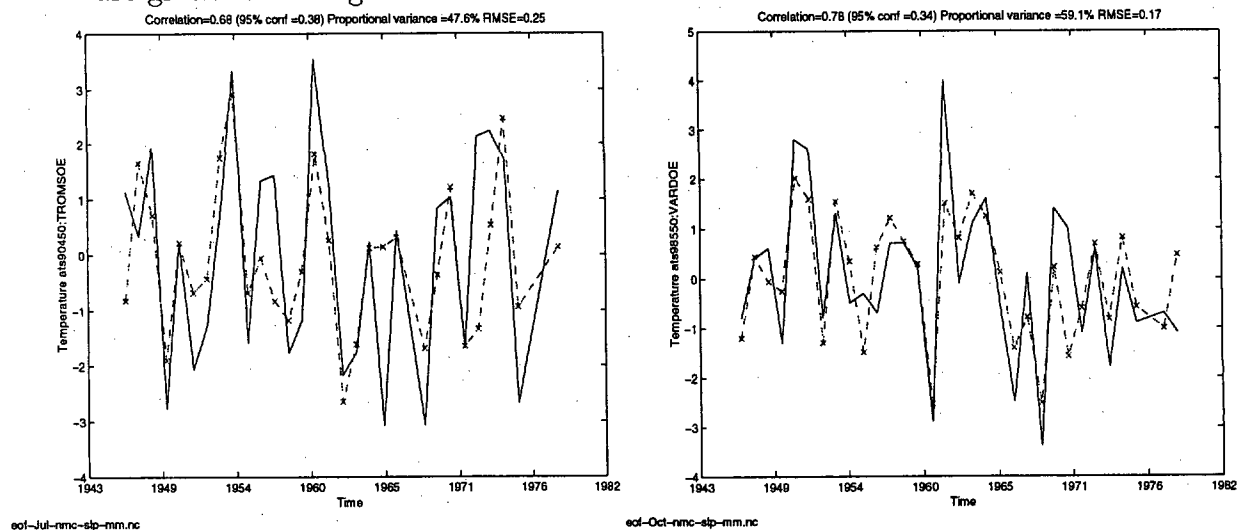


**Figure 18:** Time series of predicted July temperatures at Tromsø (left) and October temperatures at Vardø (right), employing the cross-validation method with NMC SLPs. Predictions are shown as dashed lines and observations as solid line.

eof-Jul-nmc-slp-mm.nc

eof-Oct-nmc-slp-mm.nc
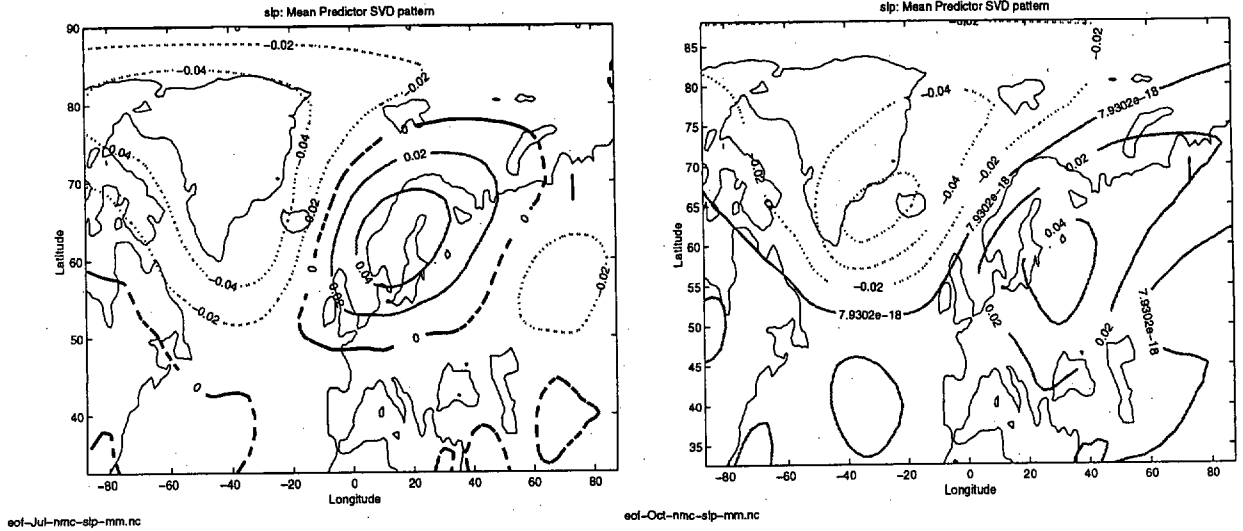
Figure 19: Same as figure 16, but for the July (left) and October (right) NMC SLP models.



eof-Jul-nmc-slp-mm.nc

eof-Oct-nmc-slp-mm.nc
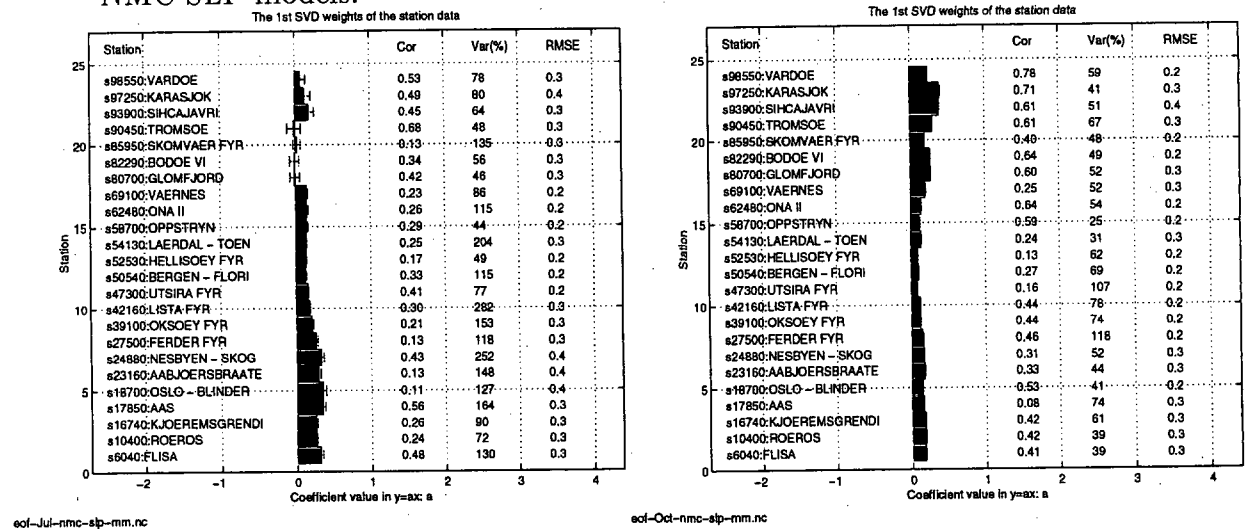
Figure 20: Same as figure 17, but for the July (left) and October (right) NMC SLP models.

scores for January: $r_{svd} = 0.75$ (Bodø, figure 15, left panel), $r_{cca} = 0.91$ (Lista); April: $r_{svd} = 0.66$ (Ås, figure 15, right panel), $r_{cca} = 0.67$ (Flisa); July: $r_{svd} = 0.68$ (Tromsø, figure 18, left panel), $r_{cca} = 0.79$ (Hellisøy fyr); October: $r_{svd} = 0.78$ (Vardø, figure 18, right panel), $r_{cca} = 0.88$ (Tromsø)). The leading January SVD SLP predictor pattern (figure 16, left panel) resembled the corresponding CCA pattern, but the April SVD pattern had much less north-south dipole character than the corresponding CCA structure (figure 16, right panel). Furthermore, the main features in the leading SVD predictor patterns for July and October were different to their CCA equivalents. The July CCA pattern described largest anomalies north of Scotland when the SVD predictors indicated strongest variability over Scandinavia (figure 19, left panel). In October, the primary feature in the CCA predictor structure was the large weights over the British Channel, but the SVD results where characterised by strongest anomalies over eastern Greenland and Iceland (figure 19, right panel).

The different leading predictor field features may suggest that more than one SLP pattern has a connection with the Norwegian temperatures. It was shown in *Benestad* (1998a) that several SLP patterns had high correlation with the Norwegian temperatures (at different locations).

The January and October models gave high correlation scores for several locations while only one station of the April and July predictions obtained a cross-validation coefficient above 0.60 (figures 17 and 20). The worst January CCA prediction was found at Vardø with r=0.00, while the SVD model also made worst prediction for Vardø, but with a higher correlation score of r=0.28. The worst SVD cross-validation correlation scores for April, July and October, however, were lower than those of the corresponding CCA models. The large skill score differences between the stations may indicate that the models only were good over limited regions. In April, July and October the CCA model predictions were less 'sensitive' to the location and in January more sensitive than the SVD predictions. The July SVD predictions for Tromsø were associated with a small leading predictand weight which was not significantly different from zero. Both the CCA and SVD October models gave best predictions in the north.

## 4.2   The UEA models

Figure 21 shows the predictions using an SLP model based on the UEA data for January (left panel) and July (right panel). The analysis of the cross-validation results demonstrated that UEA model had lower skill scores than for the corresponding NMC model predictions, although the best UEA predictions were for Nesbyen and Flisa while the best NMC predictions were
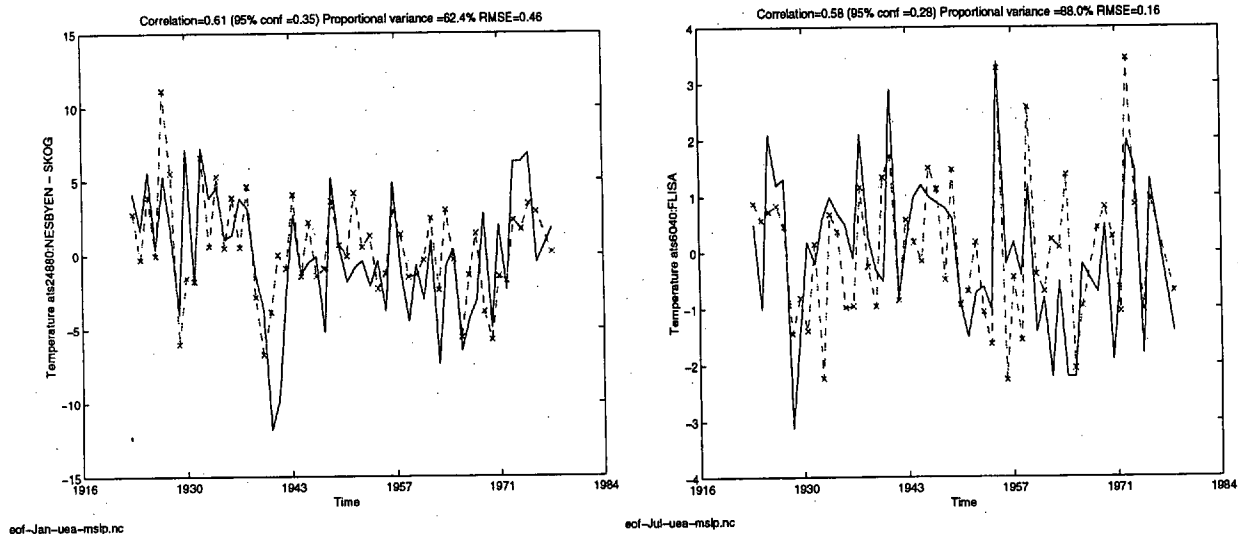
Figure 21: Time series of predicted January temperatures at Nesbyen (left) and July temperatures for Flisa (right), employing the cross-validation method with UEA SLPs. The predictions are shown as a dashed line and the observations as a solid line.



Figure 22: The mean leading January SVD UEA SLP pattern associated with the land surface temperatures.

The 1st SVD weights of the station data (January)

| Station | Cor | Var(%) | RMSE |
|---|---|---|---|
| s98550:VARDOE | 0.05 | 334 | 0.4 |
| s97250:KARASJOK | 0.31 | 49 | 0.6 |
| s93900:SIHCAJAVRI | 0.39 | 84 | 0.5 |
| s90450:TROMSOE | 0.25 | 336 | 0.5 |
| s85950:SKOMVAER FYR | 0.03 | 826 | 0.4 |
| s82290:BODOE VI | 0.38 | 259 | 0.4 |
| s80700:GLOMFJORD | 0.33 | 330 | 0.5 |
| s69100:VAERNES | 0.22 | 170 | 0.5 |
| s62480:ONA II | 0.42 | 398 | 0.4 |
| s58700:OPPSTRYN | 0.10 | 173 | 0.5 |
| s54130:LAERDAL - TOEN | 0.09 | 141 | 0.6 |
| s52530:HELLISOEY FYR | 0.29 | 307 | 0.4 |
| s50540:BERGEN - FLORI | 0.29 | 297 | 0.5 |
| s47300:UTSIRA FYR | 0.41 | 311 | 0.4 |
| s42160:LISTA FYR | 0.26 | 298 | 0.6 |
| s39100:OKSOEY FYR | 0.34 | 275 | 0.5 |
| s27500:FERDER FYR | 0.38 | 131 | 0.4 |
| s24880:NESBYEN - SKOG | 0.61 | 62 | 0.5 |
| s23160:AABJOERSBRAATE | 0.40 | 96 | 0.4 |
| s18700:OSLO - BLINDER | 0.16 | 154 | 0.6 |
| s17850:AAS | 0.23 | 101 | 0.6 |
| s16740:KJOEREMSGRENDI | 0.30 | 115 | 0.5 |
| s10400:ROEROS | 0.51 | 74 | 0.5 |
| s6040:FLISA | 0.31 | 77 | 0.6 |

Coefficient value in y=ax: a

eof-Jan-uea-mslp.nc

The 1st SVD weights of the station data (July)

| Station | Cor | Var(%) | RMSE |
|---|---|---|---|
| s98550:VARDOE | 0.29 | 54 | 0.2 |
| s97250:KARASJOK | 0.46 | 42 | 0.3 |
| s93900:SIHCAJAVRI | 0.55 | 42 | 0.2 |
| s90450:TROMSOE | 0.37 | 50 | 0.3 |
| s85950:SKOMVAER FYR | 0.34 | 77 | 0.2 |
| s82290:BODOE VI | 0.48 | 48 | 0.2 |
| s80700:GLOMFJORD | 0.47 | 44 | 0.2 |
| s69100:VAERNES | 0.40 | 50 | 0.2 |
| s62480:ONA II | 0.33 | 108 | 0.2 |
| s58700:OPPSTRYN | 0.31 | 45 | 0.2 |
| s54130:LAERDAL - TOEN | 0.30 | 39 | 0.2 |
| s52530:HELLISOEY FYR | 0.29 | 94 | 0.2 |
| s50540:BERGEN - FLORI | 0.43 | 53 | 0.2 |
| s47300:UTSIRA FYR | 0.23 | 67 | 0.2 |
| s42160:LISTA FYR | 0.37 | 60 | 0.2 |
| s39100:OKSOEY FYR | 0.14 | 42 | 0.2 |
| s27500:FERDER FYR | 0.28 | 51 | 0.2 |
| s24880:NESBYEN - SKOG | 0.37 | 60 | 0.2 |
| s23160:AABJOERSBRAATE | 0.34 | 47 | 0.2 |
| s18700:OSLO - BLINDER | 0.05 | 48 | 0.2 |
| s17850:AAS | 0.40 | 59 | 0.2 |
| s16740:KJOEREMSGRENDI | 0.40 | 66 | 0.2 |
| s10400:ROEROS | 0.30 | 27 | 0.2 |
| s6040:FLISA | 0.58 | 88 | 0.2 |

Coefficient value in y=ax: a

eof-Jul-uea-mslp.nc

Figure 23: Same as figure 17, but for the January (left) and July (right) UEA SLP models.

found at Bodø and Tromsø.

Both January SVD and CCA SLP predictor pattern had strong weights over Iceland, however, the SVD pattern also included weights with opposite polarity and maximum weights over the British Channel (figure 22, left panel). In July, the UEA SVD predictor pattern, shown in the right panel of figure 22, described a prominent west-east dipole pattern with strongest anomalies over Iceland while the corresponding CCA pattern indicated a combination of a north-south and east-west dipoles with maximum weights over Scandinavia. The best UEA SVD SLP model prediction scores were systematically lower than the best scores of the corresponding CCA models (figure 23 and table 2; ref *Benestad* (1998a)), and the locations with the highest correlation scores were different for the SVD model and the CCA model. In July, the CCA model gave best predictions at Flisa with r=0.79 and a variance score of 73% while the SVD model was associated with a lower correlation score (Flisa: r=0.58) but a better description of the temperature variance (88%). The January SVD UEA SLP model, on the other hand, only 'reproduced' 62% of the temperature variability at Nesbyen (Glomfjord: 330%) while the CCA model could 'account for' 86% at Glomfjord (Nesbyen: 65%).
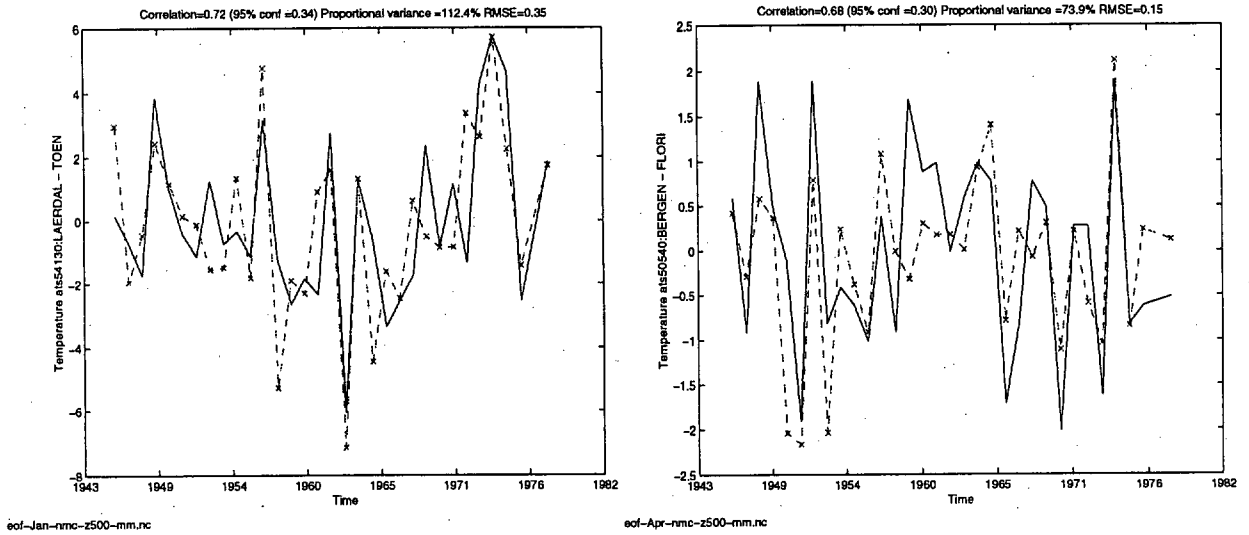
Figure 24: Time series of predicted January temperatures at Lærdal (left) and April temperatures for Bergen (right), employing the cross-validation method with NMC z(500hPa). The predictions are shown as a dashed line and the observations as a solid line.



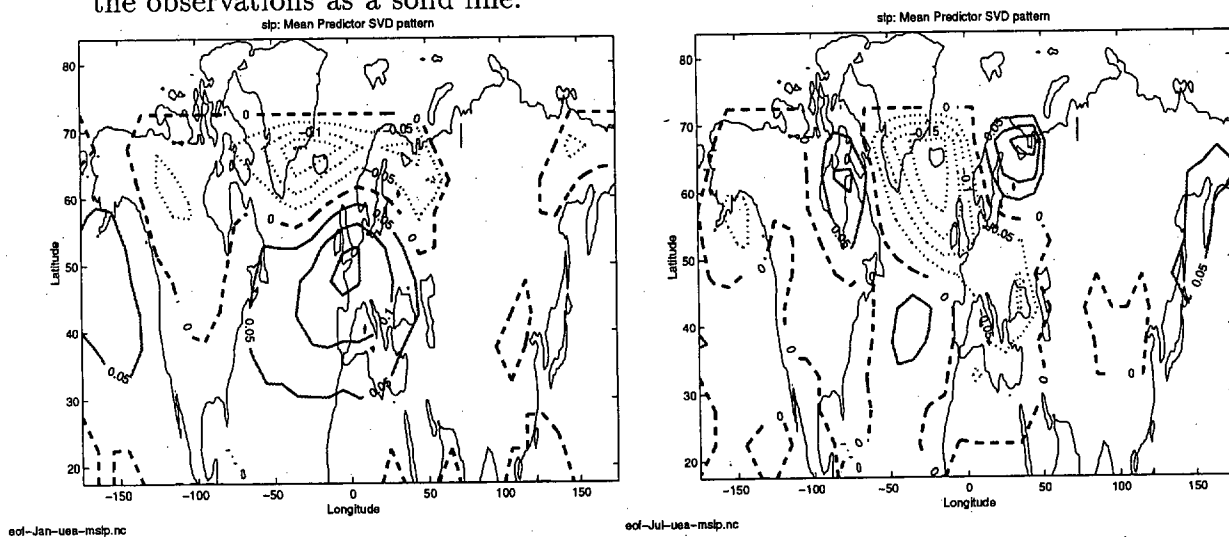Figure 25: The mean leading January (left) and April (right) SVD NMC z(500hPa) patterns associated with the land surface temperatures.

The 1st SVD weights of the station data

| Station | Cor | Var(%) | RMSE |
|---|---|---|---|
| s98550:VARDOE | 0.18 | 380 | 0.5 |
| s97250:KARASJOK | 0.49 | 33 | 0.7 |
| s93900:SIHCAJAVRI | 0.36 | 37 | 0.6 |
| s90450:TROMSOE | 0.40 | 253 | 0.5 |
| s85950:SKOMVAER FYR | 0.22 | 225 | 0.4 |
| s82290:BODOE VI | 0.40 | 230 | 0.5 |
| s80700:GLOMFJORD | 0.51 | 215 | 0.4 |
| s69100:VAERNES | 0.35 | 82 | 0.5 |
| s62480:ONA II | 0.42 | 280 | 0.4 |
| s58700:OPPSTRYN | 0.15 | 194 | 0.6 |
| s54130:LAERDAL - TOEN | 0.72 | 112 | 0.4 |
| s52530:HELLISOEY FYR | 0.17 | 274 | 0.5 |
| s50540:BERGEN - FLORI | 0.25 | 209 | 0.6 |
| s47300:UTSIRA FYR | 0.24 | 241 | 0.4 |
| s42160:LISTA FYR | 0.52 | 97 | 0.3 |
| s39100:OKSOEY FYR | 0.48 | 215 | 0.5 |
| s27500:FERDER FYR | 0.22 | 119 | 0.5 |
| s24880:NESBYEN - SKOG | 0.53 | 58 | 0.6 |
| s23160:AABJOERSBRAATE | 0.33 | 62 | 0.5 |
| s18700:OSLO - BLINDER | 0.26 | 145 | 0.6 |
| s17850:AAS | 0.31 | 81 | 0.6 |
| s16740:KJOEREMSGRENDI | 0.24 | 55 | 0.6 |
| s10400:ROEROS | 0.09 | 35 | 0.7 |
| s6040:FLISA | 0.46 | 59 | 0.6 |

Coefficient value in y=ax: a

eof-Jan-nmc-z500-mm.nc

The 1st SVD weights of the station data

| Station | Cor | Var(%) | RMSE |
|---|---|---|---|
| s98550:VARDOE | 0.64 | 83 | 0.2 |
| s97250:KARASJOK | 0.58 | 45 | 0.3 |
| s93900:SIHCAJAVRI | 0.62 | 54 | 0.3 |
| s90450:TROMSOE | 0.55 | 59 | 0.2 |
| s85950:SKOMVAER FYR | 0.10 | 80 | 0.2 |
| s82290:BODOE VI | 0.58 | 35 | 0.2 |
| s80700:GLOMFJORD | 0.21 | 26 | 0.2 |
| s69100:VAERNES | 0.27 | 28 | 0.2 |
| s62480:ONA II | 0.53 | 54 | 0.1 |
| s58700:OPPSTRYN | 0.31 | 87 | 0.2 |
| s54130:LAERDAL - TOEN | 0.20 | 41 | 0.2 |
| s52530:HELLISOEY FYR | 0.38 | 81 | 0.2 |
| s50540:BERGEN - FLORI | 0.68 | 74 | 0.1 |
| s47300:UTSIRA FYR | 0.32 | 110 | 0.2 |
| s42160:LISTA FYR | 0.42 | 78 | 0.2 |
| s39100:OKSOEY FYR | 0.24 | 57 | 0.2 |
| s27500:FERDER FYR | 0.34 | 31 | 0.2 |
| s24880:NESBYEN - SKOG | 0.34 | 42 | 0.2 |
| s23160:AABJOERSBRAATE | 0.45 | 44 | 0.2 |
| s18700:OSLO - BLINDER | 0.46 | 29 | 0.2 |
| s17850:AAS | 0.44 | 34 | 0.2 |
| s16740:KJOEREMSGRENDI | 0.41 | 43 | 0.3 |
| s10400:ROEROS | 0.43 | 28 | 0.2 |
| s6040:FLISA | 0.60 | 37 | 0.2 |

Coefficient value in y=ax: a

eof-Apr-nmc-z500-mm.nc

Figure 26: The mean leading January (left) and April (right) predictand weights for the land surface temperatures. The empty black boxes show the weights from a model trained on the whole time series. The error bars indicate the standard deviation and hence the spread in samples of each coefficient. The correlation results from the cross-validation analysis are given on the right hand side.

Correlation=0.57 (95% conf =0.33) Proportional variance =109.9% RMSE=0.18

Correlation=0.54 (95% conf =0.35) Proportional variance =265.7% RMSE=0.39

eof-Jul-nmc-z500-mm.nc

eof-Oct-nmc-z500-mm.nc

Figure 27: Time series of predicted July temperatures at Bergen (left) and October temperatures for Værnes (right), employing the cross-validation method with NMC z(500hPa). The predictions are shown as a dashed line and the observations as a solid line.

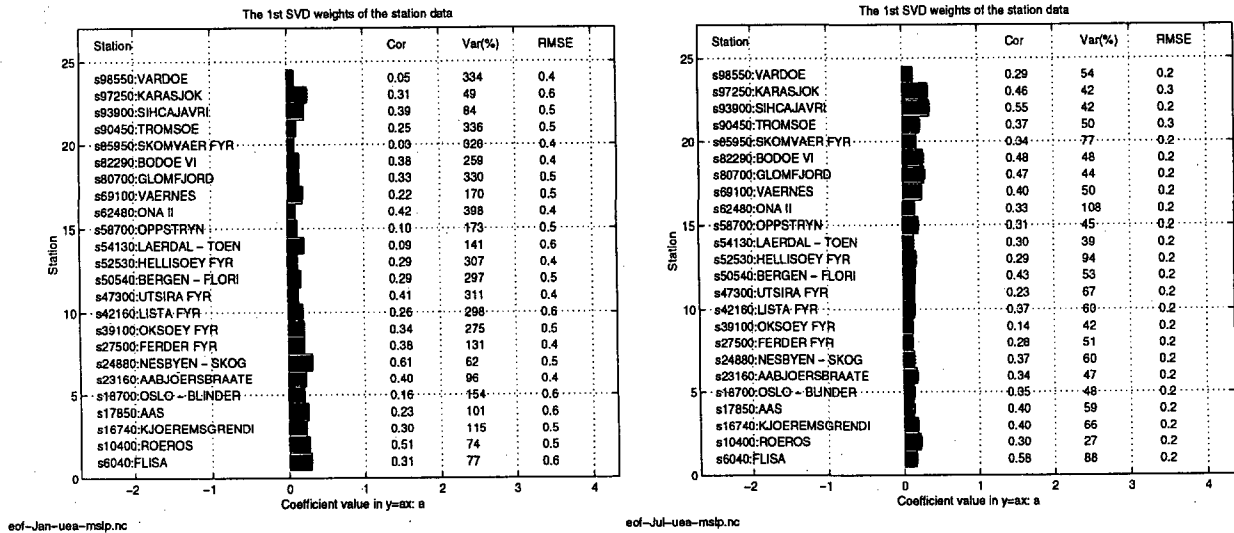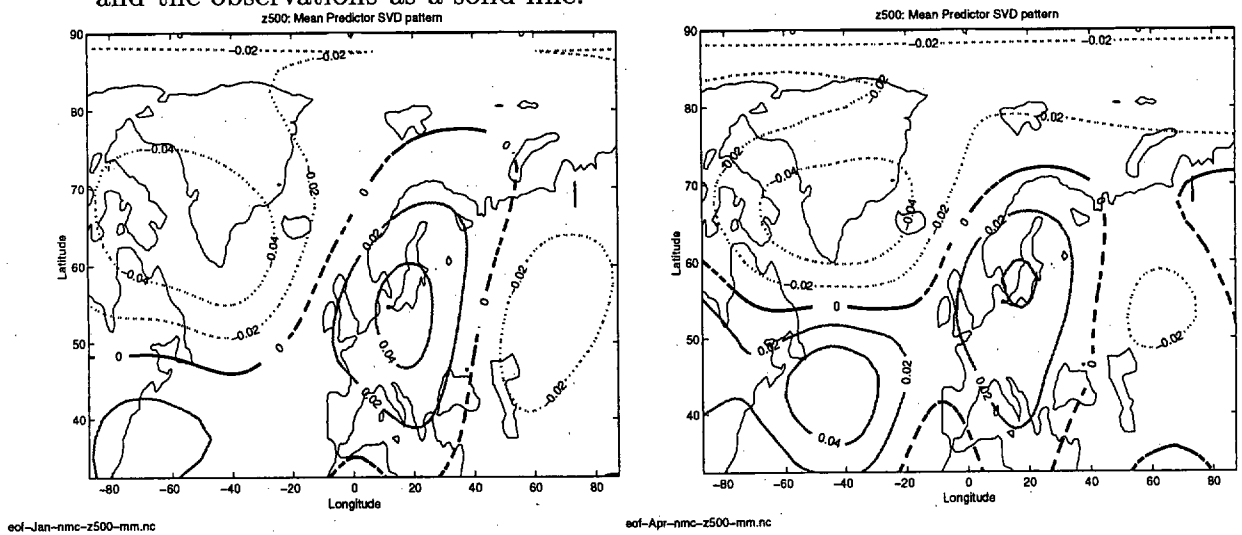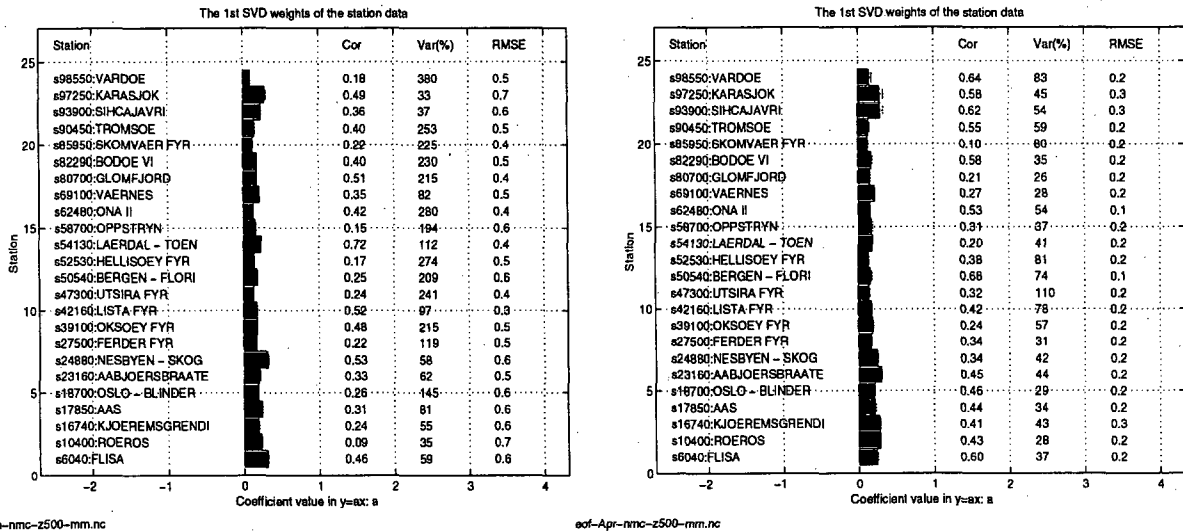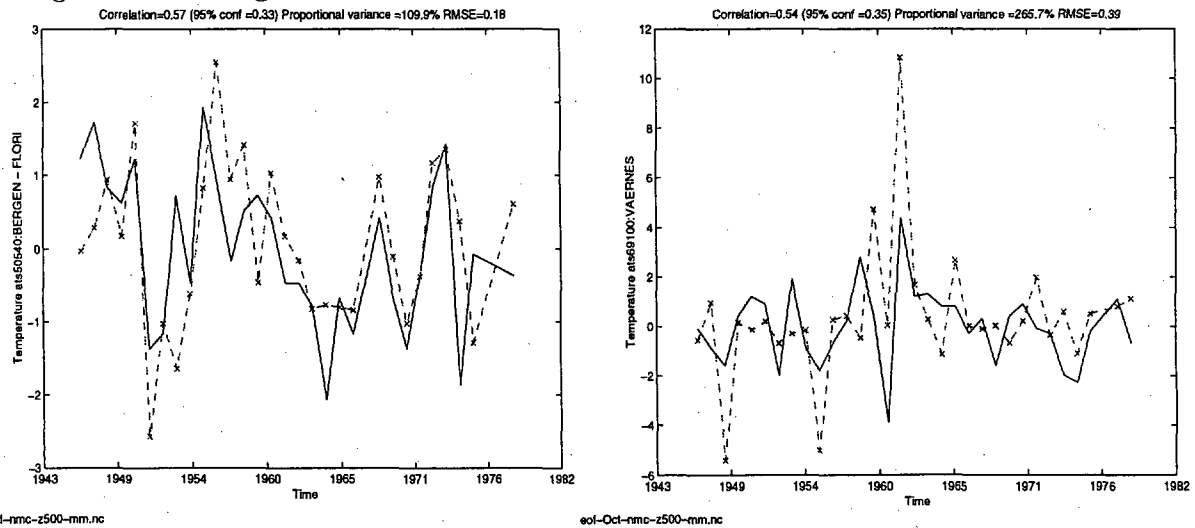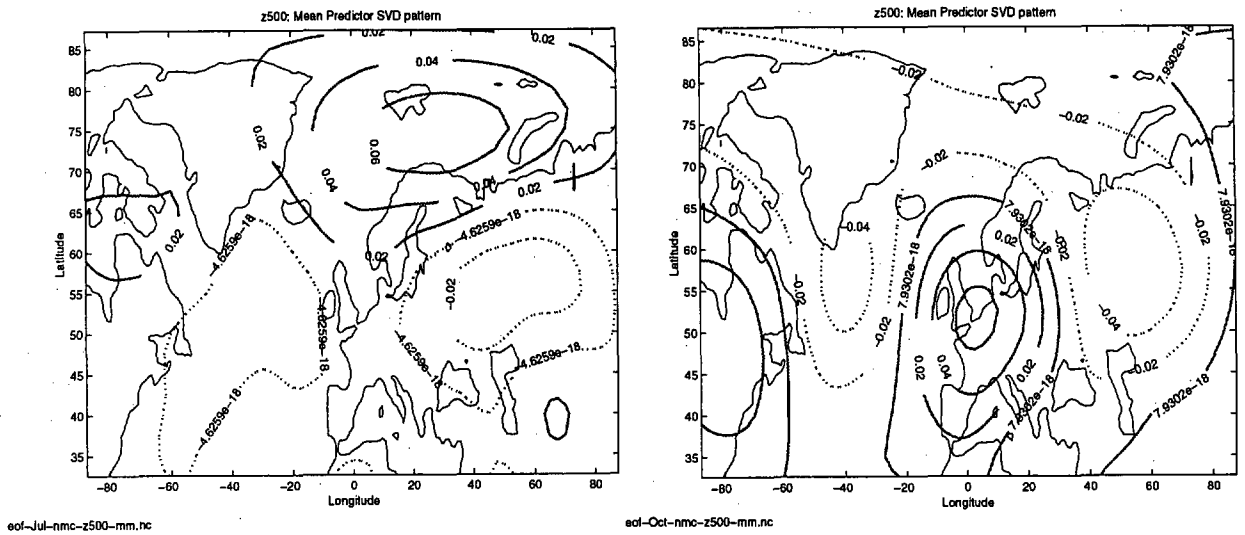Figure 28: The mean leading July SVD NMC z(500hPa) pattern associated with the land surface temperatures..
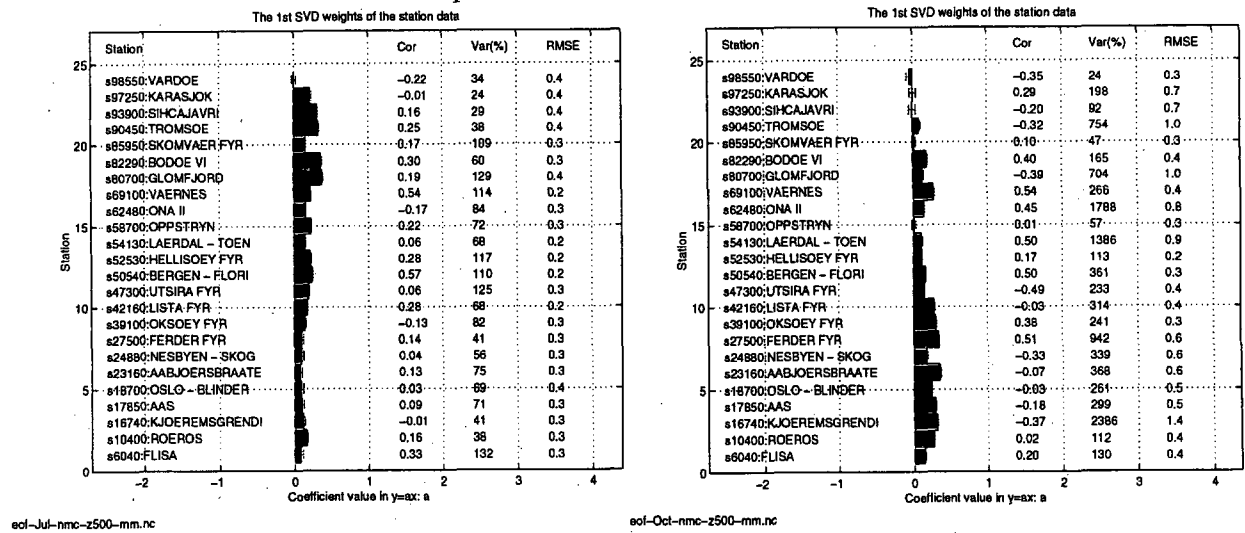


Figure 29: Same as for figure 32, but for the July (left) and October (right) NMC 500 hPa geopotential height models.

# 5   Geopotential Height Models

The results from the cross-validation predictions using the NMC ds195.5 500 hPa geopotential height, z(500hPa), as predictors are shown in the figures 24 to 29, and it is evident that the SVD z(500hPa) models were capable of predicting most of the temperature variability. The correlation scores were lower than for the CCA models, and the variance of the best prediction (Lærdal: 112%, figure 24 left panel) was slightly too high for January and 74% in Bergen for April (figure 24 right panel). The January, April, and October leading predictor patterns (figure 25 and figure 28, right panel) were similar to their corresponding CCA patterns (*Benestad*, 1998a), but the SVD July predictor pattern (figure 28, left panel) differed from the corresponding CCA pattern by showing stronger weights over eastern Russia and weaker weights over the North Atlantic.

The July SVD prediction for Bergen, shown in the left panel of figure 27, indicates a slight overestimation of the variance while the predicted variance for the October prediction was almost too large by a factor of 3. The cross-validation correlation skills were systematically lower than the scores of the corresponding CCA models (figures 26 and 29).

# 6   The 500hPa Temperature Models

The 500hPa temperature models were not discussed in *Benestad* (1998a) because the model calibration period was too short[4], as the 500hPa temperature record started as late as 1962 and the calibration period stopped in 1978 when the Skomvær fyr record ended[5]. The SVD models are not as restricted by the calibration record length as the CCA models, and it was possible to test SVD models based on the 500hPa temperature despite the short time series.

In general, the SVD T(500hPa) cross-validation prediction scores were high, and the 500hPa temperature fields were promising for the use of downscaling although longer calibration and cross-validation periods may modify these scores (table 3). The predictions in figures 30 and 33 demonstrate that the SVD T(500hPa) models captured the most important surface temperature anomalies, although the extreme values usually were exaggerated or underestimated. The leading SVD predictor patterns, shown in figures 31

---

[4]The estimate of the square root of the covariance matrices become complex (*Benestad*, 1998a).

[5]By only including stations with observations up to present, the calibration period for the 500hPa temperatures may be sufficiently long for use in CCA models.

Correlation=0.97 (95% conf =0.48) Proportional variance =41.7% RMSE=0.42

Correlation=0.86 (95% conf =0.53) Proportional variance =330.1% RMSE=0.22

eof-Jan-nmc-t500-mm.nc

eof-Apr-nmc-t500-mm.nc
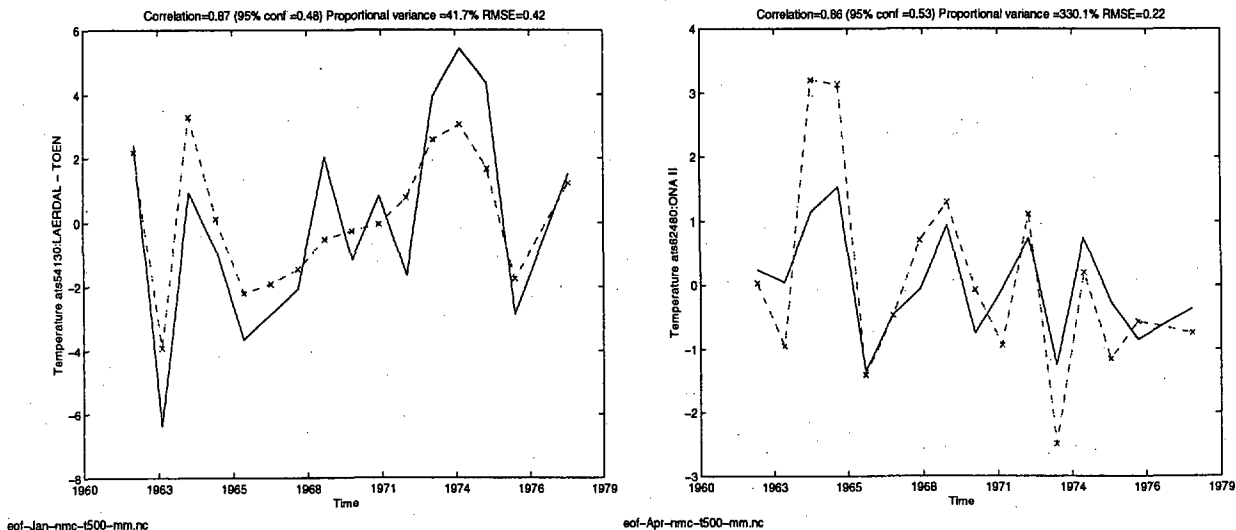
Figure 30: Time series of predicted January temperatures at Lærdal (left) and April temperatures for Ona (right), employing the cross-validation method with NMC T(500hPa). The predictions are shown as a dashed line and the observations as a solid line.

t500: Mean Predictor SVD pattern

t500: Mean Predictor SVD pattern

eof-Jan-nmc-t500-mm.nc

eof-Apr-nmc-t500-mm.nc

Figure 31: The mean leading January (left) and April (right) SVD NMC T(500hPa) patterns associated with the land surface temperatures.

The 1st SVD weights of the station data

| Station | Cor | Var(%) | RMSE |
|---|---|---|---|
| s98550:VARDOE | 0.38 | 199 | 0.5 |
| s97250:KARASJOK | 0.73 | 108 | 0.9 |
| s93900:SIHCAJAVRI | 0.67 | 117 | 0.8 |
| s90450:TROMSOE | 0.44 | 175 | 0.7 |
| s85950:SKOMVAER FYR | 0.48 | 482 | 0.7 |
| s82290:BODOE VI | 0.75 | 180 | 0.5 |
| s80700:GLOMFJORD | 0.51 | 120 | 0.6 |
| s69100:VAERNES | 0.40 | 95 | 0.8 |
| s62480:ONA II | 0.31 | 461 | 0.8 |
| s58700:OPPSTRYN | 0.58 | 148 | 0.6 |
| s54130:LAERDAL – TOEN | 0.87 | 42 | 0.4 |
| s52530:HELLISOEY FYR | 0.12 | 181 | 0.7 |
| s50540:BERGEN – FLORI | 0.11 | 117 | 0.8 |
| s47300:UTSIRA FYR | -0.07 | 339 | 1.0 |
| s42160:LISTA FYR | -0.05 | 103 | 0.9 |
| s39100:OKSOEY FYR | 0.58 | 165 | 0.7 |
| s27500:FERDER FYR | 0.37 | 157 | 0.8 |
| s24880:NESBYEN – SKOG | 0.49 | 42 | 1.0 |
| s23160:AABJOERSBRAATE | 0.31 | 58 | 0.9 |
| s18700:OSLO – BLINDER | 0.34 | 158 | 1.0 |
| s17850:AAS | 0.42 | 42 | 0.8 |
| s16740:KJOEREMSGRENDI | 0.00 | 37 | 1.0 |
| s10400:ROEROS | -0.34 | 34 | 1.5 |
| s6040:FLISA | 0.68 | 44 | 0.9 |

eof-Jan-nmc-t500-mm.nc

The 1st SVD weights of the station data

| Station | Cor | Var(%) | RMSE |
|---|---|---|---|
| s98550:VARDOE | 0.03 | 319 | 0.5 |
| s97250:KARASJOK | 0.25 | 56 | 0.4 |
| s93900:SIHCAJAVRI | 0.10 | 11 | 0.4 |
| s90450:TROMSOE | -0.16 | 187 | 0.3 |
| s85950:SKOMVAER FYR | -0.16 | 214 | 0.4 |
| s82290:BODOE VI | 0.21 | 144 | 0.4 |
| s80700:GLOMFJORD | 0.37 | 142 | 0.3 |
| s69100:VAERNES | 0.39 | 91 | 0.3 |
| s62480:ONA II | 0.86 | 330 | 0.2 |
| s58700:OPPSTRYN | 0.36 | 82 | 0.4 |
| s54130:LAERDAL – TOEN | 0.49 | 33 | 0.3 |
| s52530:HELLISOEY FYR | 0.08 | 317 | 0.4 |
| s50540:BERGEN – FLORI | 0.20 | 121 | 0.4 |
| s47300:UTSIRA FYR | 0.11 | 524 | 0.4 |
| s42160:LISTA FYR | 0.34 | 290 | 0.5 |
| s39100:OKSOEY FYR | 0.07 | 249 | 0.6 |
| s27500:FERDER FYR | 0.39 | 103 | 0.4 |
| s24880:NESBYEN – SKOG | 0.14 | 167 | 0.5 |
| s23160:AABJOERSBRAATE | 0.55 | 148 | 0.4 |
| s18700:OSLO – BLINDER | 0.26 | 148 | 0.5 |
| s17850:AAS | 0.49 | 142 | 0.4 |
| s16740:KJOEREMSGRENDI | 0.28 | 61 | 0.4 |
| s10400:ROEROS | 0.48 | 94 | 0.4 |
| s6040:FLISA | -0.03 | 78 | 0.4 |

eof-Apr-nmc-t500-mm.nc

Figure 32: The mean leading January (left) and April (right) predictand weights for the land surface temperatures. The empty black boxes show the weights from a model trained on the whole time series. The error bars indicate the standard deviation and hence the spread in samples of each coefficient. The correlation results from the cross-validation analysis are given on the right hand side.

Correlation=0.85 (95% conf =0.55) Proportional variance =120.0% RMSE=0.35

Correlation=0.81 (95% conf =0.56) Proportional variance =116.5% RMSE=0.16

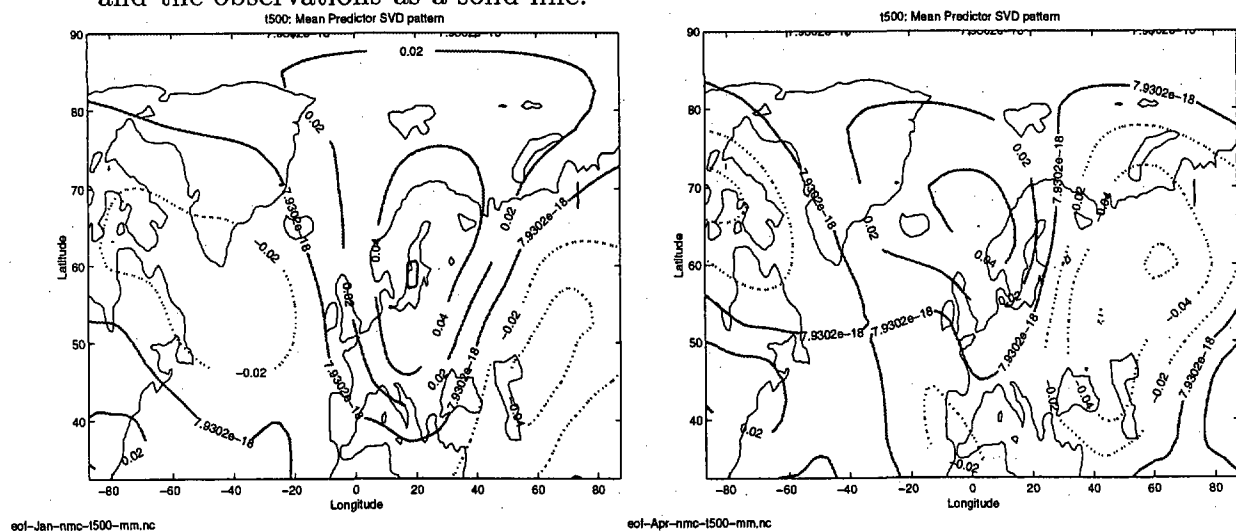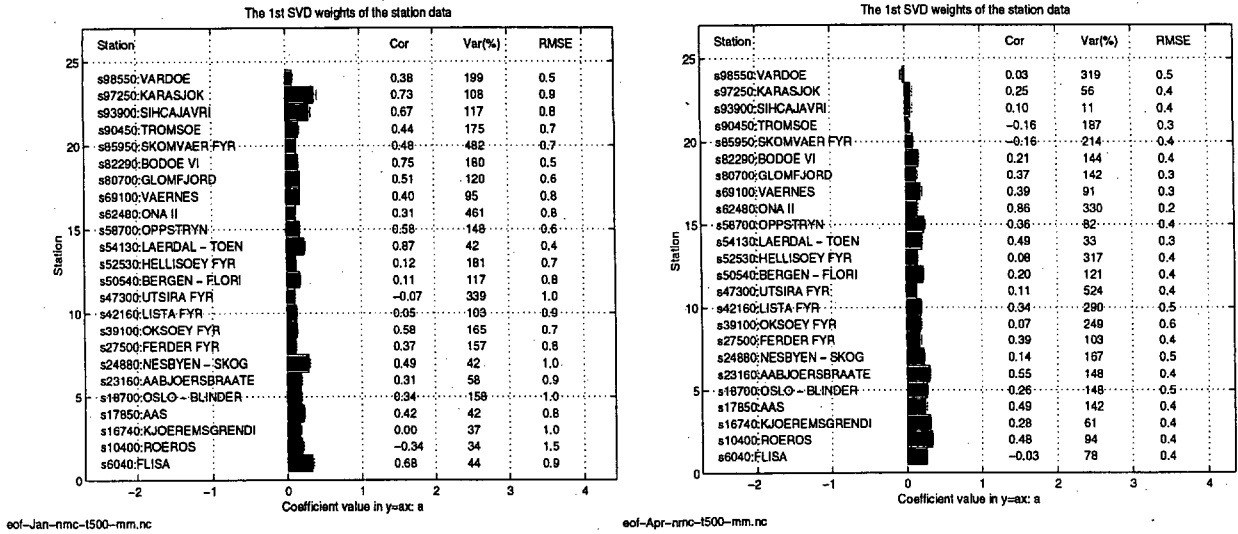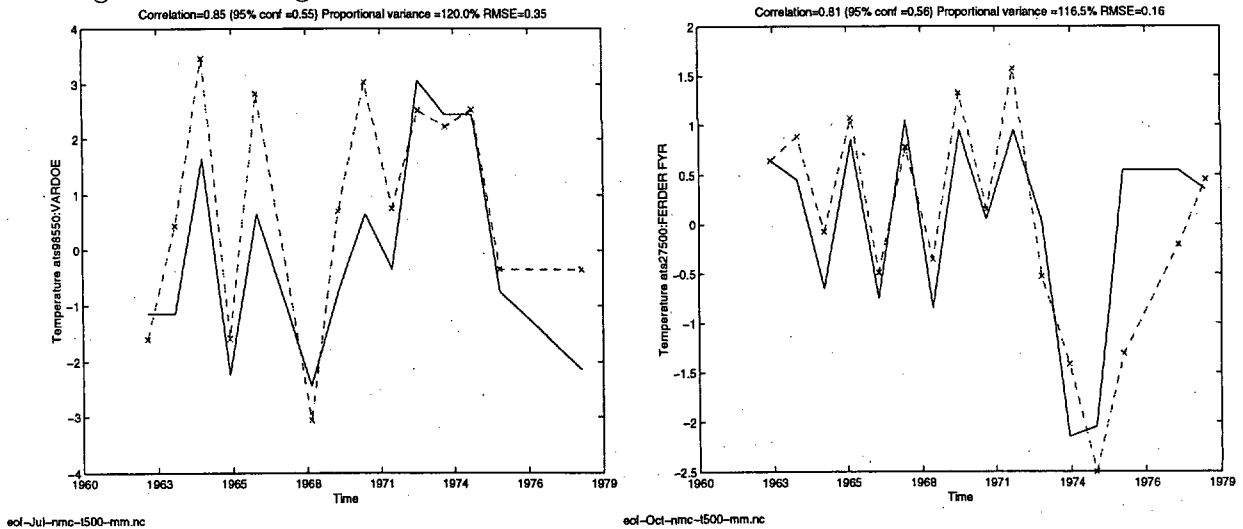eof-Jul-nmc-t500-mm.nc

eof-Oct-nmc-t500-mm.nc

Figure 33: Time series of predicted July temperatures at Ferder fyr (left) and October temperatures for Ferder fyr (right), employing the cross-validation method with NMC T(500hPa). The predictions are shown as a dashed line and the observations as a solid line.
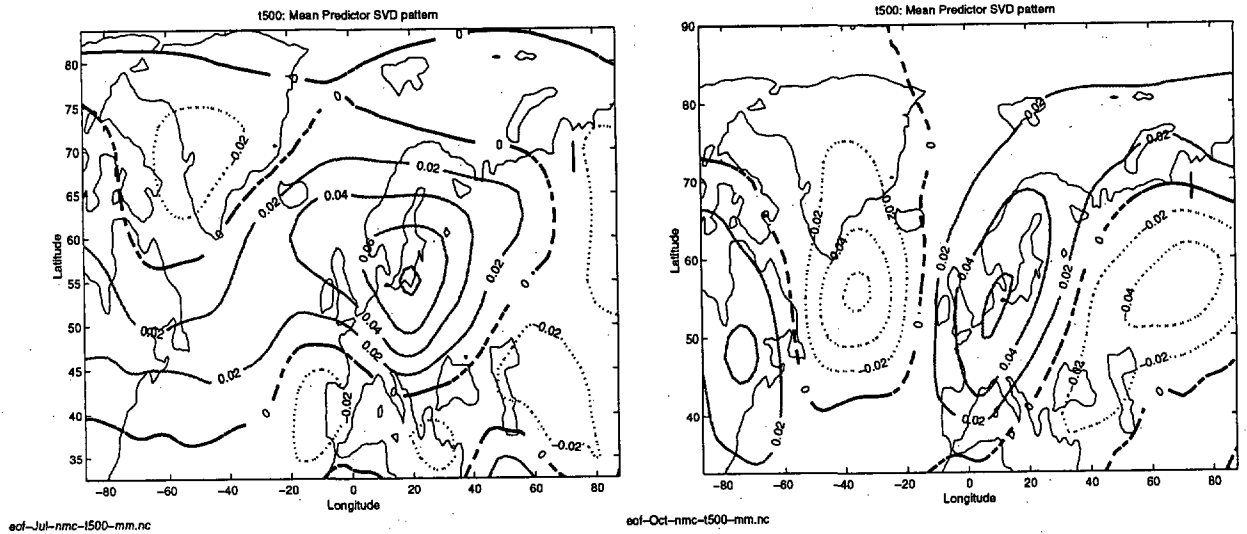
Figure 34: The mean leading July SVD NMC T(500hPa) pattern associated with the land surface temperatures.
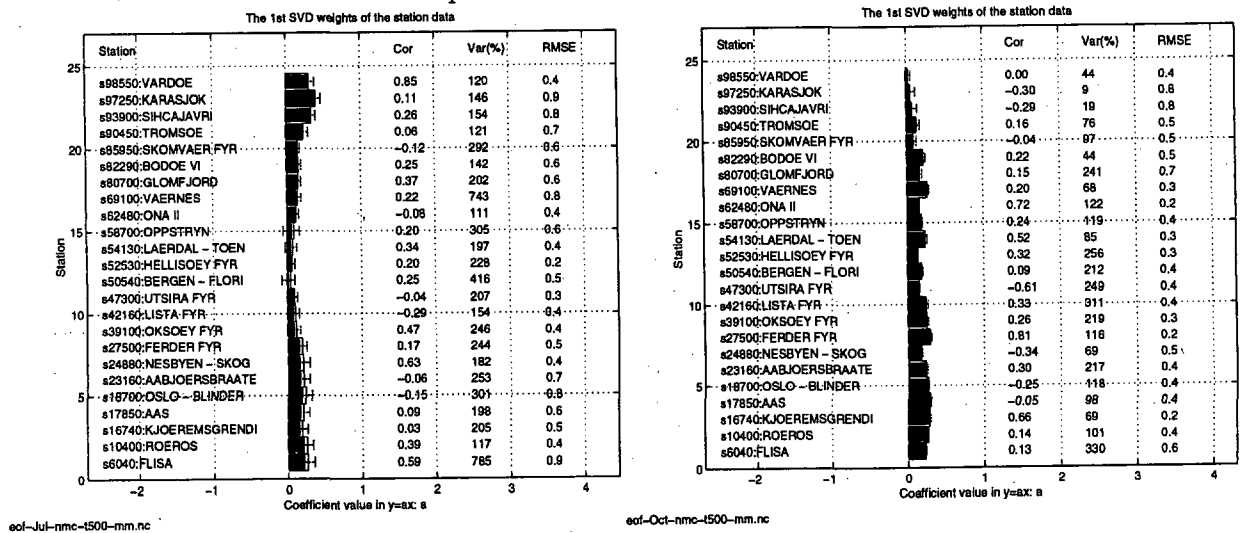


Figure 35: Same as for figure 32, but for the July (left) and October (right) NMC 500 hPa temperature models.

and 34, had largest weights over Scandinavia, suggesting that the monthly mean temperatures had a significant "barotropic" structure below the 500 hPa level. The prediction scores for the different stations in figures 32 and 35 indicated large differences between the correlation scores of the 'best' and 'worst' station. In January, the highest correlation score was found at Lærdal with r=0.87 and lowest correlation at Røros with r=-0.34. The 'worst' predictions were found at Tromsø and Skomvær fyr in April (r=-0.16), Lista fyr in July (r=-0.29), and Utsira fyr in October (r=-0.61). It is unlikely that the low prediction scores are a result of non-barotropic temperature structures due to local inversion. The most probable explanation for the bad predictions for a number of locations may be that maximising the covariance between temperatures of some 'privileged' stations and the large scale patterns causes a reduction in prediction skill of the predictands at the 'less privileged' stations. The SVD predictions were in other words sensitive to the location.

# 7 Discussion

A number of SVD models were constructed and their prediction skill scores were analysed. The main conclusion from the analysis was that the SVD models in general gave similar results as the CCA models discussed in *Benestad* (1998a). However, the CCA model cross-validation correlation scores were systematically higher than the SVD correlation scores, which is not surprising as the CCA models are optimised with respect to the correlation between the predictands and predictors.

Differences in the leading SVD and CCA predictor SLP patterns suggest that more than one SLP structure are important for the Norwegian temperatures. Likewise, several types of geopotential height anomalies were related to Norwegian surface temperature anomalies.

The station mean variance of CCA predictions were usually lower than the mean variance predicted by the SVD models which were closer to 100%, however, the SVD predictions were associated with large uncertainties for the prediction of variance at single stations, especially at stations with low cross-validation correlation scores. The SVD models may therefore only give a good prediction of the mean temperature variance for the whole of Norway when used for downscaling of a future global climate change scenario. The CCA models, on the other hand, may be more appropriate for the prediction of the variance at specific locations, but will not account for all the temperature variability. It is dangerous to scale the predicted variance according to the ratio of predicted-to-observed variance during the calibration or cross-

Table 1: Model scores

| EOFs included | Maximum correlation location (independent data) | Minimum RMSE (predictand) | Smallest correlation ('Worst prediction') |
|---|---|---|---|
| Regional SST<br>1 2 3<br>6 7 8 | Optimal CCA predictors<br>FERDER FYR<br>r= 0.65<br>rmse= 0.3 | January<br>HELLISØY FYR<br>r= 0.44<br>rmse= 0.2 | CCASVD<br>BODØ<br>r= 0.04<br>rmse= 0.4 |
| Regional SST<br>1 2 5<br>10 11 18<br>19 | Optimal SVD predictors<br>OSLO - BLINDER<br>r= 0.68<br>rmse= 0.29 | January<br>HELLISØY FYR<br>r= 0.51<br>rmse= 0.22 | TROMSØ<br>r= -0.16<br>rmse= 0.34 |
| Regional SST<br>1 2 4<br>7 | Optimal SVD predictors<br>ÅS<br>r= 0.47<br>rmse= 0.40 | April<br>VARDØ<br>r= 0.11<br>rmse= 0.24 | ÅBJØRSBRÅTE<br>r= -0.24<br>rmse= 0.55 |
| Regional SST<br>1 2 3<br>4 6 | Optimal SVD predictors<br>OPPSTRYN<br>r= 0.43<br>rmse= 0.26 | July<br>SKOMVÆR FYR<br>r= -0.03<br>rmse= 0.25 | LISTA FYR<br>r= -0.39<br>rmse= 0.44 |
| Regional SST<br>1 7 | Optimal SVD predictors<br>OKSØY FYR<br>r= 0.44<br>rmse= 0.36 | October<br>SKOMVÆR FYR<br>r= 0.17<br>rmse= 0.22 | KJØREMSGRENDI<br>r= -0.29<br>rmse= 0.60 |
| Norh Atlantic SST<br>1 2 6<br>8 9 11 | Optimal SVD predictors<br>FLISA<br>r= 0.70<br>rmse= 0.40 | January<br>VARDØ<br>r= 0.46<br>rmse= 0.22 | HELLISØY FYR<br>r= 0.23<br>rmse= 0.28 |

Table 2: Model scores

| EOFs included | Maximum correlation location (independent data) | Minimum RMSE (predictand) | Smallest correlation ('Worst prediction') |
|---|---|---|---|
| NCAR SLP<br>1 4 5<br>7 8 9<br>11 13 20 | Optimal SVD predictors<br>OKSØY FYR<br>r= 0.72<br>rmse= 0.23 | January<br>SKOMVÆR FYR<br>r= 0.63<br>rmse= 0.16 | VARDØ<br>r= 0.37<br>rmse= 0.21 |
| NCAR SLP<br>1 2 3<br>8 9 10<br>11 | Optimal SVD predictors<br>ONA II<br>r= 0.48<br>rmse= 0.11 | April<br>ONA II<br>r= 0.48<br>rmse= 0.11 | UTSIRA FYR<br>r= -0.13<br>rmse= 0.18 |
| NCAR SLP<br>1 2 3 6<br>8 9 10<br>12 13 15 | Optimal SVD predictors<br>ÅBJØRSBRÅTE<br>r= 0.61<br>rmse= 0.16 | July<br>NESBYEN - SKOG<br>r= 0.56<br>rmse= 0.16 | ONA II<br>r= 0.06<br>rmse= 0.18 |
| NCAR SLP<br>1 2 3<br>4 5 6<br>7 8 19 | Optimal SVD predictors<br>ONA II<br>r= 0.77<br>rmse= 0.12 | October<br>ONA II<br>r= 0.77<br>rmse= 0.12 | NESBYEN - SKOG<br>r= 0.34<br>rmse= 0.21 |
| NMC SLP<br>1 2 3 4<br>5 6 7 8<br>9 17 19 | Optimal SVD predictors<br>BODØ VI<br>r= 0.75<br>rmse= 0.23 | January<br>HELLISØY FYR<br>r= 0.67<br>rmse= 0.19 | VARDØ<br>r= 0.28<br>rmse= 0.26 |
| NMC SLP<br>1 3 7<br>8 9 11<br>15 16 | Optimal SVD predictors<br>ÅS<br>r= 0.66<br>rmse= 0.19 | April<br>UTSIRA FYR<br>r= 0.21<br>rmse= 0.17 | BERGEN - FLORI<br>r= -0.27<br>rmse= 0.27 |
| NMC SLP<br>1 2 3<br>7 8 10 | Optimal SVD predictors<br>TROMSØ<br>r= 0.68<br>rmse= 0.25 | July<br>UTSIRA FYR<br>r= 0.41<br>rmse= 0.18 | OSLO - BLINDER<br>r= 0.11<br>rmse= 0.41 |
| NMC SLP<br>1 2 4<br>5 7 10<br>15 20 | Optimal SVD predictors<br>VARDØ<br>r= 0.78<br>rmse= 0.17 | October<br>ONA II<br>r= 0.64<br>rmse= 0.16 | ÅS<br>r= 0.08<br>rmse= 0.32 |

## Table 3: Model scores

| EOFs included | Maximum correlation location (independent data) | Minimum RMSE (predictand) | Smallest correlation ('Worst prediction') |
|---|---|---|---|
| UEA SLP 1 3 4 | Optimal SVD predictors NESBYEN - SKOG r= 0.61 rmse= 0.46 | January ONA II r= 0.42 rmse= 0.35 | SKOMVÆR FYR r= 0.03 rmse= 0.37 |
| UEA SLP 1 2 3 4 6 9 19 | Optimal SVD predictors ONA II r= 0.58 rmse= 0.11 | April ONA II r= 0.58 rmse= 0.11 | UTSIRA FYR r= -0.06 rmse= 0.17 |
| UEA SLP 1 2 3 4 7 9 14 | Optimal SVD predictors FLISA r= 0.58 rmse= 0.16 | July FLISA r= 0.58 rmse= 0.16 | OKSØY FYR r= 0.14 rmse= 0.19 |
| UEA SLP 1 2 3 4 5 6 7 8 9 | Optimal SVD predictors BODØ VI r= 0.82 rmse= 0.14 | October OKSØY FYR r= 0.66 rmse= 0.12 | UTSIRA FYR r= 0.39 rmse= 0.13 |

validation period because the variance discrepancy reflects the part of the temperature signal which is not related to the predictor[6]. One possibility may be to represent the predictands, Y, as the sum of the contribution from the large scale circulation and a stochastic (first-order Markov chain) term, $\eta$, according to $Y = X + \eta$, and that the stochastic term accounts for the remaining of the variance in the cross-validation results. It is possible that the variance explained by the $\eta$-term may change with a global warming, and the question whether the stochastic term is stationary is one source of uncertainty for this kind of modelling.

Although the October SSTs appeared to be unconnected with the Norwegian temperatures, the October SVD predictions 'described' nearly 100% of the total variance. It is questionable whether the October SVD predictions of the temperature variance are credible, and this issue ought to be resolved before the SVD are to be used as downscaling models for future climate change scenarios.

---

[6]In fact, we learned from the cross-validation results that part (about a half) of the temperature variability was *unrelated* to the predictands. There is no guarantee that in a global warming situation the variance due to this unrelated part will change proportionally to the related part.

Table 4: Model scores

| EOFs included | Maximum correlation location (independent data) | Minimum RMSE (predictand) | Smallest correlation ('Worst prediction') |
|---|---|---|---|
| NMC $\Phi(500hPa)$ <br> 1 2 3 <br> 6 18 | Optimal SVD predictors <br> LÆRDAL - TØN <br> r= 0.72 <br> rmse= 0.35 | January <br> LISTA FYR <br> r= 0.52 <br> rmse= 0.35 | RØROS <br> r= 0.09 <br> rmse= 0.74 |
| NMC $\Phi(500hPa)$ <br> 1 2 4 <br> 5 6 8 <br> 9 11 12 | Optimal SVD predictors <br> BERGEN - FLORI <br> r= 0.68 <br> rmse= 0.15 | April <br> ONA II <br> r= 0.53 <br> rmse= 0.13 | SKOMVÆR FYR <br> r= 0.10 <br> rmse= 0.19 |
| NMC $\Phi(500hPa)$ <br> 1 5 6 <br> 10 13 | Optimal SVD predictors <br> BERGEN - FLORI <br> r= 0.57 <br> rmse= 0.18 | July <br> BERGEN - FLORI <br> r= 0.57 <br> rmse= 0.18 | VARDØ <br> r= -0.22 <br> rmse= 0.40 |
| NMC $\Phi(500hPa)$ <br> 1 14 | Optimal SVD predictors <br> VÆRNES <br> r= 0.54 <br> rmse= 0.39 | October <br> HELLISØY FYR <br> r= 0.17 <br> rmse= 0.23 | UTSIRA FYR <br> r= -0.49 <br> rmse= 0.35 |
| NMC T(500hPa) <br> 1 2 4 <br> 6 10 20 | Optimal SVD predictors <br> LÆRDAL - TØN <br> r= 0.87 <br> rmse= 0.42 | Januar <br> LÆRDAL - TØN <br> r= 0.87 <br> rmse= 0.42 | RØROS <br> r= -0.34 <br> rmse= 1.48 |
| NMC T(500hPa) <br> 1 3 6 <br> 8 9 | Optimal SVD predictors <br> ONA II <br> r= 0.86 <br> rmse= 0.22 | April <br> ONA II <br> r= 0.86 <br> rmse= 0.22 | TROMSØ <br> r= -0.16 <br> rmse= 0.32 |
| NMC T(500hPa) <br> 1 2 3 | Optimal SVD predictors <br> VARDØ <br> r= 0.85 <br> rmse= 0.35 | July <br> HELLISØY FYR <br> r= 0.20 <br> rmse= 0.25 | LISTA FYR <br> r= -0.29 <br> rmse= 0.43 |
| NMC T(500hPa) <br> 1 6 8 <br> 10 | Optimal SVD predictors <br> FERDER FYR <br> r= 0.81 <br> rmse= 0.16 | October <br> FERDER FYR <br> r= 0.81 <br> rmse= 0.16 | UTSIRA FYR <br> r= -0.61 <br> rmse= 0.41 |

Table 5: Summary of best model skills for the different models and different seasons. The score should not be directly compared as the location with highest scores varied with model and seasons. The cross-validation period for the NMC models was shorter than the for the other models, which may also give misleading results in a model score comparison.

| Month | Local SST | NCAR SLP | NMC SLP | UEA SLP | NMC $z$ | NMC $T_{500hPa}$ | Max/Min |
|-------|-----------|----------|---------|---------|---------|------------------|---------|
| Jan | 0.68 | 0.72 | 0.75 | 0.61 | 0.72 | 0.87 | 0.87 / 0.61 |
| Apr | 0.47 | 0.48 | 0.66 | 0.58 | 0.68 | 0.86 | 0.86 / 0.47 |
| Jul | 0.43 | 0.61 | 0.68 | 0.58 | 0.57 | 0.85 | 0.85 / 0.43 |
| Oct | 0.44 | 0.77 | 0.78 | 0.82 | 0.54 | 0.81 | 0.82 / 0.44 |
| avg. | 0.51 | 0.65 | 0.71 | 0.65 | 0.63 | 0.85 | |

Table 6: Summary of best CCA model skills for the different models and different seasons. The score should not be directly compared as the location with highest scores varied with model and seasons. The cross-validation period for the sea ice models and the NMC models was shorter than the for the other models, which may also give misleading results in a model score comparison.

| Month | Local SST | N.Atl. SST | NCAR SLP | NMC SLP | UEA SLP | NMC Z | Max/Min |
|-------|-----------|------------|----------|---------|---------|-------|---------|
| Jan | 0.72 | 0.75 | 0.84 | 0.91 | 0.89 | 0.91 | 0.89 / 0.64 |
| Apr | 0.65 | 0.66 | 0.66 | 0.67 | 0.60 | 0.81 | 0.82 / 0.60 |
| Jul | 0.61 | 0.48 | 0.72 | 0.79 | 0.79 | 0.89 | 0.90 / 0.48 |
| Oct | 0.48 | 0.37 | 0.86 | 0.88 | 0.83 | 0.93 | 0.94 / 0.37 |
| avg. | 0.62 | 0.57 | 0.77 | 0.81 | 0.78 | 0.89 | |

Table 7: Summary of 24-station mean model skills for the different models and different seasons. The cross-validation period for the NMC models was shorter than the for the other models, which may also give misleading results in a model score comparison.

| Month | Local SST | NCAR SLP | NMC SLP | UEA SLP | NMC $z$ | NMC $T_{500hPa}$ | Max/Min |
|-------|-----------|----------|---------|---------|---------|------------------|---------|
| Jan | 0.36 | 0.59 | 0.54 | 0.29 | 0.35 | 0.38 | 0.59 / 0.29 |
| Apr | 0.12 | 0.23 | 0.33 | 0.27 | 0.42 | 0.25 | 0.42 / 0.12 |
| Jul | 0.06 | 0.38 | 0.33 | 0.37 | 0.14 | 0.20 | 0.38 / 0.06 |
| Oct | -0.02 | 0.55 | 0.44 | 0.57 | 0.05 | 0.13 | 0.57 / -0.02 |
| avg. | 0.13 | 0.44 | 0.41 | 0.38 | 0.23 | 0.24 | |

Table 5 summarises the main model results, showing greatest correlation scores for the different models and different seasons. For comparison, the corresponding CCA results are shown in table 6. The SST, geopotential and T(500hPa) models produced the best predictions during January. The SLP models were the least skillful during April while the best skill scores of the SST, z(500hPa) and T(500hPa) model dipped to a minimum during October. A summary of the 24-station mean values is shown in figure 7. The average scores should not be taken too literally because the stations are distributed unevenly in space. However, a comparison between table 5 and table 7 illustrates how the maximum scores are unrelated to the average scores. In other words, some models may give very good predictions over a small region but nevertheless give a poor description of the climate for other parts of Norway. This was especially the case for the NMC 500hPa height and temperature models.

The cases where the standard deviation of the correlation scores was high, or the difference between the best and worst skill scores was of same magnitude as the best skill score, suggested that the empirical models sometimes only were good for limited regions. Thus, the large spread in prediction skill may be interpreted as an indication that too many stations were included in the predictand data set, and that different models ought to be used for different parts of Norway. A physical explanation for this is that some circulation patterns only affect the local climate in parts of Norway. *Hanssen-Bauer & Nordli* (1998) have identified 6 climatic regions with respect to temperature in Norway, and different models may be required for each of these regions.

The SVD models were found to be inappropriate for use in seasonal forecasting as they did not predict the timing of the large anomalies very well. However, they may be useful for downscaling of future climate scenarios in the sense that they are expected to produce similar results to the CCA models, but with greater uncertainties in the prediction of the signal variance at some stations (some predictions described variances of up to 300% of the observed variability). A comparison between the results from downscaling of future climate scenarios using the two techniques can give some insight into the uncertainties associated with the empirical predictions.

# References

Benestad, R.E. 1998a. *CCA applied to Statistical Downscaling for Prediction of Monthly Mean Land Surface Temperatures: Model Documentation.* Klima 28/98. DNMI.

Benestad, R.E. 1998b. *Description and Evaluation of the Predictor Data sets used for Statistical Downscaling in the RegClim.* Klima 24/98. DNMI.

Bhatt, U.S., Alexander, M.A., Battisti, D.S., Houghton, D.D., & Keller, L.M. 1998. Atmosphere-Ocean Interaction in the North Atlantic: Near-Surface Climate Variability. *Journal of Climate*, **11**, 1615–1631.

Bretherton, C.S, Smith, C., & Wallace, J.M. 1992. An Intercomparison of Methods for finding Coupled Patterns in Climate Data. *Journal of Climate*, **5**, 541–560.

Hanssen-Bauer, I., & Nordli, P.Ø. 1998. *Annual and seasonal temperature variations in Norway 1896-1997.* Klima 25/98. DNMI.

Preisendorfer. 1988. *Principal Component Analysis in Meteorology and Oceanology.* Elsevier Science Press.

Press, W.H., Flannery, B.P., Teukolsky, S.A., & Vetterling, W.T. 1989. *Numerical Recepies in Pascal.* Cambridge University Press.

Strang, G. 1995. *Linear Algebra and its Application.* San Diego, California, USA: Harcourt Brace & Company.

Wilks, D.S. 1995. *Statistical Methods in the Atmospheric Sciences.* Orlando, Florida, USA: Academic Press.